microscopie

Anno XI - n. 1 (21) - Marzo 2014

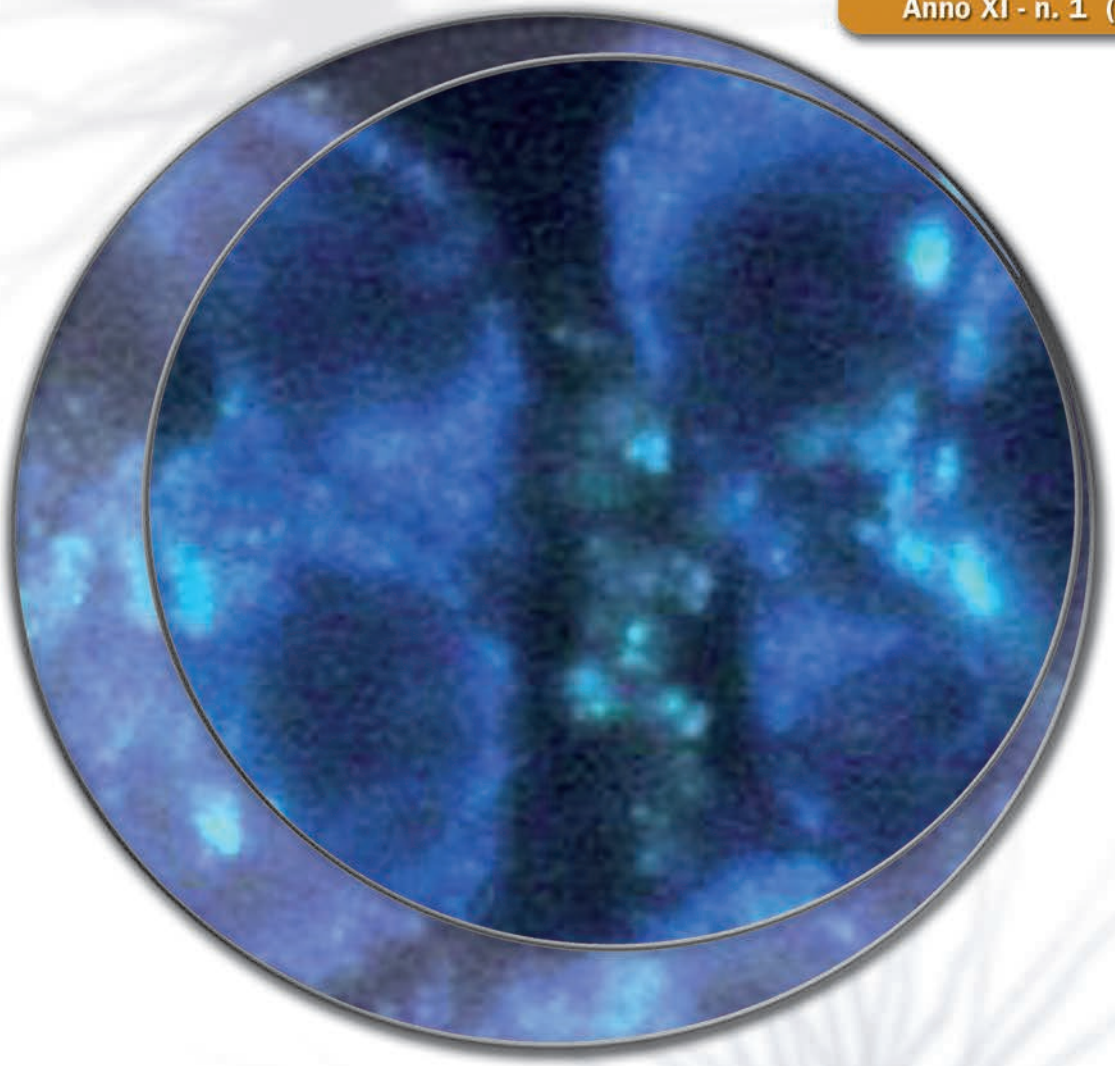

Attività SISM 2014

Bando Contributi di partecipazione al IMC 2014

Contributi scientifici del StSPM'13

Microscopist's Digest

Società Italiana
Scienze Microscopiche

www.sism.it

Periodicità Semestrale - Poste Italiane SpA - Spedizione in abbonamento Postale - D.L. 353/2003 (conv. In L. 27/02/2004 n. 46) art. 1 comma 1, DCB Milano - Taxe Perçuee

Organo Ufficiale della Società Italiana Scienze Microscopiche
http://www.sism.it

Direttore Responsabile
Manuela Malatesta

Comitato di Redazione
Consiglio Direttivo della Società Italiana Scienze Microscopiche

Editore
PAGEPress s.r.l.
via Giuseppe Belli 7
27100 Pavia, Italy
Tel. +39.0382.1751762 – Fax: +39.0382.1750481.
info@pagepress.org – www.pagepress.org

Stampa
Press Up s.r.l.
via La Spezia, 118/C 00055 - Ladispoli (RM)
Tel. e Fax: +39.076152735.

Aut. Trib. n. 688 S.P. del 26 marzo 2008

In copertina: *Autofluorescenza di cellule staminali di maiale* di Anna Cleta Croce e collaboratori.

Indice

Editoriale del Presidente 3

Editoriale del Direttore responsabile 5

Attività SISM

Verbale del CD di agosto 2013 6
Verbale della Commissione Elettorale 8
Attività promosse dalla SISM nel 2014 9
Bando Contributi di partecipazione al IMC 2014 10

Notizie

Eventi nazionali 11
Eventi internazionali 13

Microscopist's Digest 17

Contributi scientifici

Contributi scientifici del StSPM'13 18

Scanning electron microscopy in monitoring the aging of alternative materials for plastering of canvas manufactured products. 47
S. Burattini, L. Baratin, L. Borgioli, L. Sabatini, S. Orsini, V. Viti, E. Falcieri, D. De Luca

Autofluorescence and metabolic signatures in a pig model of differentiation based on induced pluripotent cells and embryonic bodies 52
A.C. Croce, G. Bottiroli, G. Santin, G. Pacchiana, P. Vezzoni, E. Di Pasquale

ISCRIZIONE

Possono iscriversi alla Società i ricercatori e gli operatori professionali comunque attivi nel campo delle diverse microscopie. Per l'iscrizione alla Società è necessario compilare la richiesta di associazione ed inviarla al Presidente. La scheda di associazione può essere compilata direttamente sul sito web della società all'indirizzo www.sism.it oppure può essere reperita in questo periodico ed inviata via fax. Le richieste verranno valutate dal Consiglio DIrettivo nella prima riunione utile e l'approvazione dei nuovi Soci sarà comunicata personalmente agli interessati. Dopo tale comunicazione il nuovo socio può procedere al pagamento della quota sociale secondo le modalità riportate sotto.

QUOTA SOCIALE

La quota sociale è di euro 35 per i soci ordinari e di euro 25 per i non strutturati. I soci non strutturati, unitamente alla quota sociale, dovranno far pervenire al Presidente della Società una dichiarazione attestante il proprio status.
Modalità di pagamento:

a) mediante carta di credito dal sito www.sism.it
b) mediante invio di un assegno bancario non trasferibile intestato a S.I.S.M.
l'assegno deve essere spedito alla Prof.ssa Elisabetta Falcieri, Dipartimento di Scienze della Terra, della Vita e dell'Ambiente (DiSTeVA), Università degli Studi di Urbino "Carlo Bo", Campus Scientifico "E. Mattei", via Ca' Le Suore 2, 61029 Urbino (PU)
c) mediante bonifico bancario intestato a S.I.S.M.
codice IBAN IT43Q0200802455000103039142
Presso Unicredit, Agenzia 3305 "Bologna Dante"
Causale: "NOME del SOCIO"

SEDE SOCIALE

Prof.ssa Elisabetta Falcieri
Dipartimento di Scienze delle Terra, della Vita e dell' Ambiente (DiSTeVA), Università degli Studi di Urbino "Carlo Bo", Campus Scientifico "E. Mattei", via Ca' le Suore 2, località Crocicchia, 61029 Urbino
Tel/Fax +39.0722.304284
E-mail: elisabetta.falcieri@uniurb.it
P.IVA 05089821002 C.F. 80181630155

SOCIETÀ ITALIANA SCIENZE MICROSCOPICHE

Richiesta di associazione

Si ricorda che le richieste di associazione verranno valutate dal Consiglio Direttivo e l'approvazione dei nuovi Soci verrà comunicata personalmente agli interessati.
Il pagamento della quota di associazione deve essere effettuato solo dopo il ricevimento della comunicazione dell'approvazione, da parte del Direttivo, della richiesta di associazione.

Il sottoscritto rischiede l'ammissione alla SISM in qualità di:

❑ Socio ordinario (35 euro)

❑ Socio non strutturato (25 euro)

Titolo, Nome e Cognome

Data di nascita

Titolo di studio e qualifica

Tipo di istituzione

❑ Università ❑ CNR ❑ Industria ❑ Commerciale ❑ Altro ente pubblico di ricerca

Istituto/Ente/Ditta

Dipartimento

Indirizzo

Città CAP

Telefono Fax E-mail

Indirizzo cui inviare la corrispondenza, se diverso dal precedente

Settore di attività

❑ Biomedico ❑ Scienza dei materiali ❑ Commerciale ❑ Altro (specificare) _____

Come deliberato nell'Assemblea Generale del 24/09/2001 ogni Socio SISM è anche Socio EMS.
Questi stessi dati saranno pertanto automaticamente inviati anche all'EMS, di cui la SISM fa parte. I dati dei Soci sono utilizzati dalla Segreteria EMS per distribuire il Notiziario in forma elettronica, per annunciare informazioni importanti come Congressi, Corsi, Scuole e per pubblicare l'Annuario dei Soci EMS.
Se si desidera che i propri dati personali non compaiano nell'annuario EMS, selezionare l'apposita opzione.

❑ Chiedo che il mio indirizzo privato non compaia nell'annuario EMS

❑ Chiedo che il mio numero di telefono/fax non compaia nell'annuario EMS

Data _____ Firma _____

Inviare via fax a:

Prof.ssa Elisabetta Falcieri
Dipartimento di Scienze della Terra, della Vita e dell'Ambiente (DiSTeVA), Università degli Studi di Urbino "Carlo Bo"
Campus Scientifico "E. Mattei", via Ca' Le Suore 2, 61029 Urbino (PU)
Tel. +39.0722.304284 Fax: +39.0722.304244

Editoriale

Cari Amici e Colleghi,

Come sapete, Il 2013 è stato l'ultimo anno della Presidenza SISM di Amelia Montone, e il 2014 sarà il primo della mia. Nel ringraziare chi mi ha dato il voto per il sostegno e per la fiducia, vorrei, a mia volta, dedicare ad Amelia il mio pensiero e la mia gratitudine. Lo scorso agosto, in occasione del Congresso di Regensburg, ha fatto a grandi linee il resoconto del suo mandato e io, che le sono stata vicina per molti anni, posso confermare con quanta dedizione, efficienza organizzativa e tenacia abbia portato avanti questa Società. Non sono infatti momenti facili né per i giovani, il cui prezioso entusiasmo va tenuto vivo, né per noi che stiamo dando tanto da tanto tempo e che non dobbiamo smettere di insegnare, stimolare, essere di esempio. Le istituzioni, grandi e piccole, vivono delle idee e della forza di coloro che ne fanno parte.
Il mio primo obiettivo sarà quello di consolidare i risultati ottenuti dalla gestione di Amelia, cercando di mantenere la vivacità e la qualità degli eventi scientifici e contando sull'efficienza organizzativa, che, in un paese dove la burocrazia rischia di soffocare anche le realtà più brillanti, una Società come la nostra può e deve ancora mantenere. Mi impegnerò affinché venga conservata la trasversalità della SISM, nella convinzione che anche chi proviene dal mondo biomedico come me, riconoscendosi nell' ambito tecnologico-strumentale e confrontandosi con chi "guarda" i materiali, possa trarne un valore aggiunto. Del resto tutti i congressi internazionali di microscopia dimostrano fortemente che questo approccio è quello migliore per far nascere cultura, innovazione, collaborazioni e risorse. Porrò particolare attenzione ai rapporti con la European Microscopy Society, importante organo di riferimento, oltreché partner in molteplici attività, come il 10th Multinational Congress on Microscopy 2011 di Urbino, in occasione del quale ho potuto conoscerne da vicino il livello, l'organizzazione e le persone.
Un mio secondo obiettivo sarà quello di favorire la partecipazione dei Soci alla vita della SISM. È vero che molti di noi sono soci di più Società Scientifiche, ma la Società Italiana di Scienze Microscopiche, oltre ad avere, da sempre, quote di iscrizione molto basse, organizza eventi improntati, virtuosamente, ad una certa semplicità e, soprattutto, prevede agevolazioni importanti per i giovani. Tutte le attività scientifiche sono infatti supportate da premi o borse di partecipazione, con cui, come accade da anni, si consente la partecipazione a giovani non strutturati, altrimenti impossibilitati. E proprio in quest'ottica, nella recente riunione del nuovo Consiglio Direttivo, abbiamo approvato l'istituzione di borse di partecipazione anche per il IMC 2014, che si terrà a Praga il prossimo settembre.
A questo proposito, mi sembra doveroso ringraziare le aziende che sponsorizzano la Società, sia istituzionalmente sia in occasione degli eventi organizzati: il loro costante contributo, su cui speriamo di poter sempre contare, è cosa preziosa.
Non posso dimenticare il nucleo di persone attive e presenti in tutte le occasioni, oltreché instancabilmente al servizio della Società…. mi riferisco a Roberto Balboni, che da sempre gestisce il sito, silenzioso strumento indispensabile per tutti noi. E non mi stancherò mai di ringraziare Manuela Malatesta, che, con grande attenzione ed entusiasmo, cura il nostro giornale *Microscopie*, fonte di informazione per tutti e preziosa palestra per i giovani che si affacciano alla ricerca microscopica. Entrambi hanno dato ancora la loro disponibilità e questo mi fa guardare al futuro con spirito costruttivo, come solo un solido gioco di squadra può consentire. E così Andrea Tombesi che, ancor di più come vicepresidente, contribuirà a mantenere la convivenza tra le microscopie, anima importante della

Editoriale

SISM. E ancora Cristiano Albonetti, con le sue microscopie a scansione di sonda, dai materiali alle scienze della vita. Conto molto, infine, sulle due nuove presenze in Consiglio Direttivo, Stefania Meschini, che conosco da tanti anni come instancabile ricercatrice dell'Istituto Superiore di Sanità e Regina Cianci, di cui ho avuto modo di apprezzare a Regensburg capacità, disponibilità e simpatia, poi confermate nell'avvio di questo impegnativo ma stimolante lavoro.
Affronto questo periodo con grande entusiasmo e fiducia: come sanno gli amici del Consiglio Direttivo, mi sono candidata con piacere, credo nella cultura e nella ricerca scientifica…. e penso che anche questo sia un modo per traghettare verso momenti migliori. A disposizione di tutti, quando e nei modi che riterrete più opportuni, vi invio i miei più cordiali saluti. Buon lavoro.

Elisabetta Falcieri

Editoriale

Cari Soci,
con questo numero inizia il mio quarto mandato in qualità di Direttore responsabile di *Microscopie*. L'esperienza di questi anni mi ha insegnato moltissimo e trovo ancora stimolante cimentarmi nel campo dell'editoria scientifica. Ringrazio, quindi, tutti coloro che mi hanno rinnovato la loro fiducia: mi impegnerò ancora una volta a fare del mio meglio per mantenere e, possibilmente, migliorare la qualità della nostra Rivista.
Con il rinnovo del Consiglio Direttivo e l'elezione di Elisabetta Falcieri come Presidente inizia un capitolo nuovo della storia della SISM, e anche *Microscopie* già subisce qualche piccolo cambiamento.
Innanzitutto, in questo numero troverete una sezione scientifica più ampia; infatti, oltre ai consueti articoli, grazie alla preziosa collaborazione di Cristiano Albonetti vengono pubblicati 14 minipaper scritti dai partecipanti al workshop *Science through Scanning Probe Microscopy (StSPM'13,)* svoltosi a Bologna nel dicembre 2013. La pubblicazione degli atti di un workshop è un'iniziativa inedita che immagino gradita a tutti i Soci e che spero si potrà replicare in occasione di altri eventi organizzati dalla nostra Società. Come ho già scritto in precedenti editoriali, uno dei miei obiettivi è implementare la sezione scientifica, ma per raggiungere questo risultato è assolutamente necessario il sostegno e la collaborazione di tutti voi!
La seconda novità è costituita dall'inaugurazione di una rubrica intitolata *Microscopist's Digest* (tanti fra noi ricordano la storica rivista *Reader's Digest*), nella quale vengono segnalati articoli di particolare interesse per le scienze microscopiche recentemente apparsi su riviste internazionali indicizzate. Invito quindi tutti i Soci a inviarmi le indicazioni bibliografiche di articoli che ritengano degni di segnalazione, accompagnate da una breve presentazione in inglese che ne sottolinei gli aspetti di originalità ed innovazione. Mi auguro che nella sua duplice valenza, divulgativa e didattica, questa nuova rubrica possa essere apprezzata sia dai microscopisti più esperti sia dalle giovani leve.
Infine, a partire da questo numero, la stampa di *Microscopie* diventa digitale: la tecnologia attuale garantisce ormai una qualità grafica del tutto comparabile a quella della stampa tradizionale e, allo stesso tempo, consente un notevole abbattimento dei costi. Per una Società, come la nostra, che vive di quote sociali e del sostegno di sponsor, ogni risparmio di gestione può significare qualche contributo in più per la partecipazione di nostri giovani agli eventi congressuali. Colgo quindi l'occasione per salutare e ringraziare la Tipografia PIME che, negli ultimi sei anni, con il suo ottimo lavoro tipografico, ha dato un contributo fondamentale alla qualità della nostra rivista.
Mi rendo conto d'aver scritto già troppo e quindi, come di consueto, chiudo con l'augurio di buona lettura.

Manuela Malatesta

Consiglio direttivo della SISM

Verbale della riunione del 28 agosto 2013

Università di Regensburg, Germania

Il giorno 28 agosto 2013, alle ore 12:30, presso l'Università di Regensburg (Germania), in occasione del MC 2013, è convocata una riunione del Consiglio Direttivo SISM, per discutere il seguente OdG:

1. Approvazione del verbale della riunione precedente.
2. Approvazione della Relazione del CD sulla gestione scientifica ed economica della SISM nel biennio 2012-2013.
3. Situazione economica della Società.
4. Approvazione della Relazione del Direttore di "Microscopie" sulla gestione scientifica della rivista
5. Valutazione candidature per MCM 2015.
6. Stato organizzativo attività SISM 2013 e valutazioni preliminari attività 2014.
7. Aggiornamenti rivista Microscopie e sito web.
8. Definizione delle modalità di voto per il rinnovo delle cariche sociali.
9. Proposta di Soci Onorari.
10. Approvazione ammissione nuovi Soci.
11. Contributi di partecipazione al MC 2013 e Premi Carla Milanesi.
12. Varie ed eventuali.

Sono presenti: *Cristiano Albonetti*, *Roberto Balboni*, *Elisabetta Falcieri*, *Manuela Malatesta*, *Amelia Montone*.
Assenti giustificati: *Rita Musetti e Andrea Tombesi*.
Presiede *Amelia Montone*; svolge le funzioni di segretario verbalizzante *Roberto Balboni*.

1. Il verbale della riunione del Direttivo del 11 febbraio 2013 viene approvato all'unanimità.
2. Il presidente Amelia Montone dà lettura della Relazione sulla gestione scientifica ed economica della Società per il biennio 2012-2013. La relazione viene approvata all'unanimità.
3. La gestione della società ha prodotto un utile che, alla fine dell'anno 2012, è dell'ordine di 15.000 €. Nell'anno in corso vi sono state le spese ordinarie ed alcune attività devono ancora essere svolte. Non si prevedono comunque variazioni di rilievo.
4. Il Direttore della rivista "Microscopie" Manuela Malatesta dà lettura della Relazione sulla gestione scientifica della rivista per il biennio 2012-2013. La Relazione viene approvata all'unanimità.
5. Per l'organizzazione del prossimo Multinational Congress on Microscopy (MCM 2015), verranno presentate le candidature di Croazia (Opatia), Serbia (Belgrado) e Ungheria (Eger). Il Direttivo raccomanda ai delegati di tener conto, nella scelta fra i candidati, della accessibilità e dei costi di partecipazione.

6. SI è conclusa nel mese di febbraio 2013, con l'effettuazione della parte pratica, la Scuola TEM in Scienza dei Materiali presso il CNR di Bologna.
   Il Workshop organizzato da R. Musetti a Udine dal titolo "Le piante: dalla morfologia alle interazioni con l'ambiente" ha avuto un ottimo successo, con circa 30 partecipanti.
   Si svolgeranno come previsto le restanti tre attività:
   - Corso Base integrato di microscopia confocale e microscopia elettronica in trasmissione, organizzato da A. Tombesi presso il CIGS dell'Università di Modena (11-13 settembre 2013).
   - Workshop di due giornate dal titolo "Science through Scanning Probe Microscopy (StSPM)", organizzato da C. Albonetti presso il CNR di Bologna (dicembre 2013).
   - Scuola base SEM e di preparativa campioni per SEM/STEM, organizzata da P. Mengucci presso il Dipartimento di Scienze e Ingegneria della Materia dell'Università di Ancona (1-3 ottobre 2013).

7. Per quanto riguarda la stampa della rivista "Microscopie", M. Malatesta propone di attivare con la tipografia la procedura di stampa digitale, che ha raggiunto un livello di qualità comparabile con la stampa analogica, e dovrebbe permettere anche un risparmio economico. Il Direttivo delibera di procedere in tal senso una volta verificata l'economicità dell'operazione.

8. Viene deliberato di procedere al voto per il rinnovo delle cariche sociali mediante posta ordinaria, così come in passato. Si dà altresì mandato al Consiglio Direttivo entrante di valutare, per future votazioni, l'allestimento della procedura di voto utilizzando il sito web.

9. Non vi sono proposte di nomina di soci onorari.

10. Approvazione ammissione nuovi Soci:
    Miriam Ascagni
    Valentina D'Oria
    Anita Giglio
    Alesssandro La Torre
    Martina Marchiori
    Stefania Meschini
    Maria Carla Panzeri
    Cristiano Rumio
    Nadia Santo
    Salvatore Valiante

11. Viste le domande pervenute, il Consiglio Direttivo delibera di assegnare sette contributi di partecipazione MC 2013, dell'importo di 700,00 € ciascuno, ai seguenti candidati:
    Dott.ssa Michela Battistelli
    Dott.ssa Giuseppina Bozzuto
    Dott. Davide Curzi
    Dott. Alessandro Maiorana
    Dott.ssa Valentina Palmieri
    Dott.ssa Sara Salucci
    Dott.ssa Eleonora Santecchia
    Sono inoltre pervenute sette domande relative al premio Carla Milanesi. Il Direttivo nominerà i due vincitori al termine del Congresso MC2013 in cui i lavori dei candidati sono stati presentati.

12. Nulla da deliberare.

Amelia Montone
Roberto Balboni
Cristiano Albonetti
Elisabetta Falcieri
Manuela Malatesta

Verbale della commissione elettorale per l'elezione delle cariche sociali della SISM per il biennio 2014-2015

L'Assemblea dei Soci della SISM, svoltasi il 29 agosto 2013 a Regensburg in occasione del Microscopy Congress 2013, ha nominato la Commissione elettorale che risulta così costituita:
Presidente : Armigliato Aldo
Membri: Quaglino Daniela, Morandi Vittorio
Amelia Montone, Presidente della Società, ha consegnato l'elenco aggiornato dei Soci aventi diritto al voto (allegato al presente verbale), secondo quanto disposto dal punto a) dell'art. 19 del Regolamento, unitamente alla schede per l'elezione del Presidente e dei Consiglieri.

I 105 Soci aventi diritto al voto hanno ricevuto per lettera la comunicazione della candidature e le schede per la votazione (copia della lettera è allegata al presente verbale) con richiesta di esprimere il proprio voto entro le ore 18 del 21 novembre 2013, secondo quanto disposto dal punto d) dell'art. 19 del Regolamento.

Alle ore 10.00 del giorno 5 dicembre 2013 si riunisce la Commissione elettorale per lo spoglio delle schede pervenute (58 per l'elezione del Presidente e 58 per l'elezione dei Consiglieri). Dopo aver verificato l'integrità delle buste contenenti le schede, le buste stesse vengono aperte e si procede allo scrutinio.

L'esito della votazione per l'elezione del Presidente è il seguente

FALCIERI Elisabetta	Voti 48
SCHEDE BIANCHE	3
SCHEDE NULLE	7

Pertanto risulta eletto quale Presidente della Società Italiana Scienze Microscopiche per il biennio 2014-2015: FALCIERI Elisabetta

L'esito della votazione per l'elezione dei Consiglieri è il seguente

ALBONETTI Cristiano	Voti 24
BALBONI Roberto	Voti 36
CIANCIO Regina	Voti 15
MALATESTA Manuela	Voti 35
MESCHINI Stefania	Voti 23
MUSETTI Rita	Voti 10
TOMBESI Andrea	Voti 37
FALCIERI Elisabetta	Voti 1
SCHEDE BIANCHE	0
SCHEDE NULLE	6

Pertanto risultano eletti quali Consiglieri della Società Italiana Scienze Microscopiche per il biennio 2014-2015:
TOMBESI ANDREA
BALBONI ROBERTO
MALATESTA MANUELA
ALBONETTI CRISTIANO
MESCHINI STEFANIA
CIANCIO REGINA

Le operazioni di scrutinio si chiudono alle ore 12.00.
Letto, approvato e sottoscritto seduta stante dai componenti della Commissione elettorale.

Dott. Armigliato Aldo
Prof.ssa Quaglino Daniela
Dott. Morandi Vittorio

Elenco delle attività promosse dalla SISM nel 2014

Scuola EELS, organizzata dal Dott. Giuseppe Nicotra dell'IMM. Il Dott. Roberto Balboni farà parte del Comitato Scientifico.
Catania, 26-28 maggio 2014

Scuola congiunta di Microscopia Confocale-STEM, presso il CIGS dell'Università di Modena, a cura del Dott. Andrea Tombesi.
Modena, fine settembre/inizio ottobre 2014

Workshop teorico-pratico su "La microscopia confocale nello studio dei mitocondri", a cura della Prof.ssa Elisabetta Falcieri.
Urbino, seconda metà di ottobre 2014

Scuola TEM in Scienza dei Materiali, organizzata dal gruppo di Microscopia Elettronica del CNR-IMM (parte teorica in Novembre 2014 e parte pratica in Febbraio 2015), a cura del Dott. Roberto Balboni.
Bologna, novembre 2014

Workshop su "La microscopia elettronica applicata allo studio dei beni culturali", a cura della Prof.ssa Elisabetta Falcieri.
Urbino, novembre 2014

E per il 2015...

Workshop su "Contributi delle microscopie allo studio delle colture cellulari", in collaborazione con l'Associazione Italiana per le Colture Cellulari, a cura della Dott.ssa Stefania Meschini.
Roma, ISS, aprile 2015

Workshop congiunto di "Microscopia elettronica e microscopia mediante luce di Sincrotrone" a cura della Dott.ssa Regina Ciancio.
Trieste, seconda metà 2015

La SISM darà inoltre il **patrocinio** ai seguenti eventi:

Celebrazione del quarantennale del CIGS di Modena, all'interno del quale si collocherà un intervento del Presidente della SISM (proposto dal Dott. A. Tombesi)

Nanomedicine 2014, organizzato, presso l'Università di Viterbo dalla Associazione Italiana per le Colture Cellulari (proposto dalla Dott.ssa S. Meschini)

S.I.S.M. Società Italiana Scienze Microscopiche

Urbino, 10-02-2014

CONTRIBUTI DI PARTECIPAZIONE AL IMC 2014

La Società Italiana Scienze Microscopiche (SISM), in collaborazione con le Aziende del settore della Microscopia, bandisce

n. **4 CONTRIBUTI** (2 del settore "biomedico" e 2 del settore "scienza dei materiali")

dell'importo di **€ 500,00** ciascuno, per favorire la partecipazione di giovani ricercatori italiani al 18th International Microscopy Congress (www.imc2014.com) che si terrà a Praga dal 7 al 12 settembre 2014.

I Contributi di partecipazione sono riservati a **ricercatori non strutturati, iscritti alla Società alla data di presentazione della domanda**.

I partecipanti devono inviare entro la data di scadenza per l'invio degli abstract al Congresso (attualmente prevista per il 5 marzo 2014):

1) Copia dell'abstract inviato al Congresso

2) Curriculum Vitae, di massimo due pagine, con autocertificazione della propria posizione lavorativa.

Ricordiamo che la scadenza per il pagamento della quota standard di iscrizione al Congresso è il 1 luglio 2014.

Per partecipare alla selezione del bando, che verrà effettuata a giudizio insindacabile del Consiglio Direttivo, **la documentazione richiesta va inviata per e-mail al Presidente della SISM, Prof.ssa Elisabetta Falcieri (elisabetta.falcieri@uniurb.it).**

PRESIDENTE
Prof.ssa Elisabetta Falcieri
Dipartimento di Scienze delle Terra, della Vita e dell' Ambiente (DiSTeVA) - Università degli Studi di Urbino Carlo Bo, Campus Scientifico "E.Mattei"
Via Ca' le Suore 2, località Crocicchia, 61029 Urbino
Tel. 0722-304284 Email: elisabetta.falcieri@uniurb.it
Sede Sociale S.I.S.M:
Dipartimento di Scienze delle Terra, della Vita e dell' Ambiente (DiSTeVA) - Università degli Studi di Urbino Carlo Bo, Campus Scientifico "E.Mattei", Via Ca' le Suore 2, località Crocicchia, 61029 Urbino
SISM P.IVA 05089821002 C.F. 80181630155

Eventi nazionali

2014

Corso Annuale di Microscopia applicata alla Micologia
Verona, 22 febbraio 2014
http://www.veronamicologica.com/uploads/documenti%20sezione%20ATTIVITA'/programma_corso_di_miscroscopia_2014_ok.pdf

La citometria dell'emoglobinuria parossistica notturna (EPN)
Napoli, 26 febbraio - 4 giugno 2014
http://biotec.casaccia.enea.it/gic/

Scuola di microscopia "life imaging"
Bologna, 5-7 marzo 2014
http://www.ior.it/sites/default/files/Programma%20definito%2022-12-13.pdf

La citometria nella ricerca di base e nella clinica
Busto Arsizio (VA), 14 marzo 2014
http://biotec.casaccia.enea.it/gic/AVVISI-fold/Corso%20La%20Citometria%20nella%20Ricerca%20di%20Base%20e%20nella%20Clinica%203-2014.pdf

Microendodontics 2014: Corso di Microendodonzia
Napoli, 21-22 marzo 2014
http://enricogalise.wordpress.com/2014/02/14/corso-di-microscopia-dott-palazzi-2122-marzo-2014/

Nanomedicine 2014
Viterbo, 17-19 settembre 2014
www.nanodrug.cnr.it

Viterbo, 17-19 September 2014

University of Tuscia

Via Santa Maria in Gradi 4, Viterbo, Italy

Diagnosis

Therapy

Theranostics

Medical devices

Nanoscopies

Nanomaterials for tissue engineering

CHAIRPERSONS

Yechezkel BARENHOLZ
Alberto DIASPRO
Giovanna MANCINI
Agnese MOLINARI

Organized by

Department of Technology and Health, Istituto Superiore di Sanità, Rome
Institute of Chemical Methodologies, CNR, Rome
http://www.nanodrug.cnr.it

Graphic by Casimo Marino Curianò SAE-ISS

Istituto Superiore di Sanità

Consiglio Nazionale Ricerche

Università degli Studi della Tuscia

iit Istituto Italiano di Tecnologia

Società Chimica Italiana

Eventi internazionali

Focus on Microscopy 2014
April 13-16, 2014
Sydney, Australia

European Light Microscopy Meeting 2014 (ELMI 2014)
May 20-23, 2014
Holmenkollen, Oslo, Norway

"3D Electron Microscopy: From Molecule to Organism"
May 22-23, 2014
UPMC, Paris, France

European Molecular Imaging Meeting - the EMIM 2014
9th annual meeting of the European Society for Molecular Imaging – ESMI
June 4-6, 2014
Antwerp, Belgium

Digital Image Processing Workshop
June 6, 2014
London, UK
Organization: Royal Microscopical Society (RMS)

Workshop on Electron Wave Imaging (Holo-Workshop)
June 9-13, 2014
Dresden, Germany

SCANDEM 2014
Specimen preparation course
Annual Conference of the Nordic Microscopy Society
June 11-13, 2014
Linköping, Sweden

Live-Cell Imaging
June 17-19, 2014
University of East Anglia, Norwich, UK

Microscience Microscopy Congress 2014 (mmc2014)
June 30 - July 3, 2014
Manchester Central, Manchester, UK
Organization: Royal Microscopical Society (RMS)

2nd FIB & Prep (Focus Ion Beam and EM Sample preparation) UK User Group Meeting
Associated meeting of mmc2014
July 1, 2014
Manchester Central, Manchester, UK

Advanced Topics in Aberration-Corrected STEM
July 4-7, 2014
SuperSTEM Laboratory, Daresbury, UK

Quantitative Analysis of Grain Size
July 17, 2014
University of York, UK
Organization: Royal Microscopical Society (RMS)

Getting the most of your Confocal
July 17-18, 2014
University of York, UK
Organization: Royal Microscopical Society (RMS)

AFMWorkshop Atomic Force Microscopy Applications Workshop
July 21-25, 2014
Liquid Crystal Institute, Kent State University, Kent, Ohio, USA

Ninth International Conference on Charged Particle Optics (CPO-9)
August 31 - September 5, 2014
Brno, Czech Republic

IMC2014
18th International Microscopy Congress
September 7-12, 2014
Prague, Czech Republic
Organization: Czechoslovak Microscopy Society (CSMS)

Geo-Materials Sample Preparation Workshop
September 11, 2014
Department of Earth Sciences, University of Oxford

XV International Conference on Electron Microscopy
September 15-18, 2014
AGH University of Science and Technology, Kraków, Poland
Organization: Polish Society for Microscopy Committee of Materials Science of the Polish Academy of Sciences

ESREF 2014
25th European Symposium on Reliability of Electron Devices, Failure Physics and Analysis
September 30 - October 2, 2014
EFUG/FIB session: Tuesday September 30, 2014
Berlin, Germany

Autumn School on Microstructural Characterization and Modelling of Thin-Film Solar Cells
November 2-7, 2014
Resort Hotel Schwielowsee, Werder (near Potsdam), Germany

Eventi internazionali

18TH INTERNATIONAL MICROSCOPY CONGRESS

MICROSCOPY FOR GLOBAL CHALLENGES
touching atoms, molecules, nanostructures and cells by multidimensional microscopy

Prague, 7 - 12 September 2014

IMC PRAGUE 2014

updated
SECOND ANNOUNCEMENT
January 2014

Important dates
5 March 2014 — Abstracts submission & early registration deadline
1 July 2014 — Standard registration deadline

CSMS
IFSM

Plenary speakers
Roger Y. Tsien - Nobel Prize laureate in chemistry, University of California San Diego, USA
Paul Midgley, Department of Materials Science and Metallurgy, University of Cambridge, UK
Kazutomo Suenaga, National Institute of Advanced Industrial Science and Technology, Japan
Xiaowei Zhuang, Howard Hughes Medical Institute, Harvard University, USA
John Spence, Arizona State University, Physics/LBNL, USA (The John Cowley Medal)
Chunlin Jia, Ernst Ruska - Centre Jülich, Germany and International Centre for Dielectric Research, Xi'an Jiaotong University, China (The Hatsujiro Hashimoto Medal)
Alasdair Steven, National Institute of Arthritis and Musculoskeletal and Skin Diseases, USA (The Eduard Kellenberger Medal)
Ondrej L. Krivanek, Nion Company and Arizona State University, USA (The V. Ellis Cosslett Medal)

Scientific program
58 sessions in Instrumentation and Techniques, Materials Science, Life Sciences and Interdisciplinary.

Other highlights
IFSM symposium, IFSM school, pre-and post-congress activities, lunch workshops
Congress party "In Art Nouveau" in the historical Prague Municipal House
Extensive commercial exhibition with novel instruments

Congress secretariat: Guarant International, Na Pankráci 17, 140 21 Praha 4, Czech Republic, Tel. +420 284 001 444, Fax : +420 284 001 448, E-mail: info@imc2014.com

www.imc2014.com

DGE DEUTSCHE GESELLSCHAFT FÜR ELEKTRONENMIKROSKOPIE

Deutsche Gesellschaft für Elektronenmikroskopie e.V.

(German Society for Electron Microscopy)

announces the

ERNST RUSKA PRIZE 2015

for outstanding achievements in the field of electron microscopy.

The Deutsche Gesellschaft für Elektronenmikroskopie invites to propose candidates for the Ernst-Ruska-Prize. The prize is awarded for work carried out by younger scientists pioneering new capabilities of electron microscopy as a scientific technique through innovative instrumentation or novel methods of basic and general interest. Work carried out by pure application of existing techniques will not be considered. The eligible work should not date back more than 7 years. It must be published or it must be accepted for publication at the time of submission of the proposal.

The decision will be made by an independent committee. The Ernst-Ruska-Prize consists of a certificate, a financial award, as well as the honor of giving an *Ernst-Ruska Distinguished Lecture* at the Ceremony of Award. If a group of authors receives the award, they will be awarded jointly. The ceremony will take place at the Microscopy Conference 2015 in Göttingen, Germany, Sept. 6th- 11th, 2015.

Proposals including appraisal of the achievement, reprints or preprints, and short CV including list of publications of the authors should be received (on paper and CD) not later than November 30th, 2014, addressed to

President of DGE
Dr. Michael Laue
Robert Koch-Institut
Nordufer 20
13353 Berlin
GERMANY
E-mail: lauem (at) rki.de

Atomic structure from large-area, low-dose exposures of materials: a new route to circumvent radiation damage

Meyer J.C., Kotakoski J., Mangler C.

Ultramicroscopy, 2013(http://dx.doi.org/ 10.1016/j.ultramic.2013.11.010)

This paper deals with the difficulties in extracting structural information at the atomic/molecular level in beam radiation sensitive samples. Modern microscopes allow atomic resolution to be achieved in most samples, but this is obtained with an increased electron dose that can have detrimental effect on the sample itself. In addition to a reduction of the beam energy, to avoid knock-on effects, ionisation sensitive samples require a reduction of the beam intensity, that generally makes the noise the dominant part of the image. The authors propose a statistical method that allows the extraction of structural information at the atomic level even in cases in which the features in the direct images cannot be distinguished, with the solely requirement that the features to be detected can be considered as repeated perturbations of a constant, known structure. Although not yet supported experimentally, the method is interesting in view of the present high interest in low-dimensional materials and could in principle be applied to the detection of point defects, ad-atoms or attached functional groups and adsorbed molecules.

Roberto Balboni - CNR, Bologna

Ultrastructural detection of photosensitizing molecules by fluorescence photoconversion of diaminobenzidine

Pellicciari C., Giagnacovo M., Cisterna B., Costanzo M., Croce A.C., Bottiroli G., Malatesta M.

Histochem. Cell Biol. 139: 863-871, 2013

Photosensitizers are chemical compounds whose cytotoxic action is due to their capability to convert light energy for inducing oxidative processes: on their action is based the moderately invasive therapeutic procedure called photodynamic therapy. Following light irradiation, photosensitizers produce oxidizing chemical species (singlet oxygen, free radicals or reactive oxygen species) which can damage the cell molecular structures and induce cell death. Indirect evidence of the photosensitizer interaction with specific organelles has so far been inferred from the photodamage after irradiation, as observed by fluorescence or electron microscopy. In this article, for the first time a direct detection of the subcellular location of photosensitizing molecules was obtained at transmission electron microscopy: HeLa cells were loaded with two different fluorogenic substrates, Rose Bengal acetate or Hypocrellin B acetate, taking advantage of the photophysical properties of the intracellularly restored photosensitizing molecules to obtain the photoconversion of diaminobenzidine into an electrondense product. It was demonstrated that these photosensitizing agents are mostly internalized by endocytosis, and follow the endosomes–lysosome route, being found in endosomes, lysosomes and multivescicular bodies; diaminobenzidine deposits were also detected in the cytosol. Due to the very short half-life of the oxidizing chemical species and their consequently low mobility, diaminobenzidine deposits localize very close to the place where photoactive molecules elicited the production of reactive oxygen species upon light irradiation: thus this procedure may be foreseen as a very suitable tool for elucidating the mode of penetration of other photosensitising molecules into the cells and for tracking their dynamic intracellular relocation and organelle targeting.

Carlo Zancanaro - Università di Verona

Simultaneous detection of multiple targets for ultrastructural immunocytochemistry

Philimonenko V. V., Philimonenko A. A., Šloufová I., Hrubý M., Novotný F., Halbhuber Z., Krivjanská M., Nebesá ová J., Šlouf M., Hozák P.

Histochem. Cell Biol., 2014 (doi: 10.1007/s00418-013-1178-6)

Immunocytochemistry has been a powerful tool for at least three decades now, both at light and electron microscopy. A part from the different resolution and the presence of colours in the images there is another difference between the two applications, that is the possibility of simultaneously labelling multiple antigens. In fluorescence, three antigens are quite common and one can go up to even five or six. At EM, however, the situation is different and it is rather rare to label three antigens simultaneously. In the "roaring '80s", at the beginning of immunoelectron microscopy, some papers showed up to five antigens labelled by colloidal gold particles of varying size. However, for several reasons (including the overlapping of the distribution range of the different particles), this approach has more or less been abandoned. The paper I am suggesting here solves the problem with a radical switch of the approach. The Authors prepared a set of shape-coded metal nanoparticles which can be conjugated to antibodies or other bioreactive molecules. Using these novel nanoparticles in combination with commercial gold nanoparticles, up to five molecular targets can easily be identified simultaneously. No need to be expert electron microscopists, just have a look at the images: anybody can make the difference between a sphere, a cube or a rod. As simple as that!

Marco Biggiogera - Università di Pavia

Culturing muscle fibres in hanging drop: A novel approach to solve an old problem

Archacka K., Pozzobon M., Repele A., Rossi C.A., Campanella M., De Coppi P.

Biol. Cell 106: 72-82, 2014

The culture of skeletal muscle satellite cells in vitro represents a widely used model for investigating myogenic differentiation. However, over the years a variety of protocols for isolation, culture and analysis of satellite cells have been developed which may account, at lest in part, for the heterogeneous results published. In fact, the satellite cells obtained by mechanical disruption and/or enzymatic digestion of the muscle tissue belong to different subpopulations characterised by distinct marker expression, and by diverse proliferation, differentiation and fusion potentials. In addition, cultured satellite cells isolated from myofibres might differently react to the inducing stimuli than those exposed to the signals released in their physiological niche. To overcome these limitations, the Authors developed a novel approach to the culture of satellite cells by adapting the hanging drop system that is commonly used for inducing differentiation of embryonic stem cells. After isolating single muscle fibres together with their associated satellite cells from skeletal muscle, the hanging drop method allowed satellite cells and their niche to interact each other avoiding premature satellite cell activation and differentiation. Consequently, the behaviour of satellite cells in their natural location may be monitored for an extended period of culture time.

Manuela Malatesta - Università di Verona

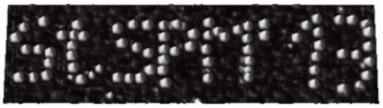

Science through Scanning Probe Microscopy (StSPM'13)

12 – 13 dicembre 2013, Bologna, CNR – Area della Ricerca

Il workshop Science through Scanning Probe Microscopy (StSPM'13), organizzato dall'Istituto per lo Studio dei Materiali Nanostrutturati (ISMN) e dalla Società Italiana di Scienze Microscopiche (SISM), in collaborazione con l'Area della Ricerca di Bologna, si proponeva come punto di incontro per microscopisti a scansione di sonda (SPM) e, considerati i 60 ricercatori partecipanti, pensiamo di esserci riusciti. Con grande piacere abbiamo registrato la partecipazione di ricercatori provenienti da molte regioni italiane, sia dal sud che dal nord, afferenti ad università, enti di ricerca e laboratori industriali, ma la cosa più importante è stata la alta partecipazione di giovani ricercatori.

StSPM'13 è stata l'occasione per illustrare i recenti avanzamenti scientifici nelle macro-aree scientifiche "Materials Science" e "Life Science", ottenuti grazie alla Microscopia a Scansione di Sonda (SPM). Sono stati presentati 25 contributi orali, di cui 8 ad invito per professori e ricercatori di chiara fama. I contributi sono stati bilanciati nelle due macro-aree e organizzati in modo che il workshop si condensasse nel pomeriggio del 12 e nella mattina del 13 dicembre. Per mantenere costante l'attenzione dei partecipanti, abbiamo alternato le discipline e, a posteriori, pensiamo sia stata una buona idea come hanno dimostrato le numerose domande alla fine di ogni presentazione. L'ambiente collaborativo e spontaneo che si è instaurato tra i partecipanti ha permesso agli studenti di sentirsi liberi di fare domande e di proporre idee e, *in ultimis*, di perdonarci i ritardi accumulati nelle singole sessioni, frutto di un eccesso di entusiasmo organizzativo e voglia di partecipazione alle discussioni.

Di fondamentale importanza per la riuscita dell'evento è stata la partecipazione e il contributo economico delle ditte SPM, sponsors dell'evento e della SISM. In tutto hanno partecipato 13 persone in rappresentanza di 16 ditte legate alla microscopia a scansione di sonda. La loro partecipazione è stata apprezzata dai partecipanti che, grazie a due sessioni speciali dedicate alle ditte, hanno potuto vedere le ultime novità commerciali in fatto di microscopi, sonde ed accessori.

Infine, seguendo lo spirito educativo della SISM, abbiamo colto l'occasione del workshop per realizzare questi proceedings su Microscopie, la rivista della società. Pur non essendo una rivista ad impatto internazionale pensiamo che i manoscritti che seguono siano, soprattutto per i ricercatori più giovani, un buon modo per imbastire la prima bozza di un manoscritto che, in futuro, diventerà sicuramente una pubblicazione internazionale.

Ringraziamo pubblicamente tutti coloro che hanno partecipato all'organizzazione e hanno supportato l'iniziativa in qualsiasi forma e, per concludere, vi aspettiamo a StSPM'16 dove, siamo convinti, parteciperete con entusiamo e nuovi risutalti scientifici.

Il comitato scientifico

Dott. Cristiano Albonetti
Dott. Francesco Valle
Prof. Fabio Biscarini

Magnetisation reversal in magnetic patterned structures by means of field-dependent MFM

M. Coïsson,[1] G. Barrera,[1,2] F. Celegato,[2] E. Enrico,[1] A. Manzin,[1] P. Tiberto,[1] F. Vinai[1]

[1]*INRIM, Electromagnetism Division, strada delle Cacce 91, 10135 Torino (TO), Italy*
[2]*Università degli Studi di Torino, Dip. di Chimica, via P. Giuria 7, 10125 Torino (TO), Italy*

Corresponding author: M. Coïsson
E-mail: m.coisson@inrim.it

Key words: MFM, patterned nanostructures, magnetisation reversal.

Introduction

Nanostructured thin films, consisting of periodically patterned ferromagnetic materials, have been extensively investigated in the last decade due to the development of magnetoelectronic devices for high-density information storage, MRAM and magnetologic [1,2]. In order to reach a complete understanding of their properties, the magnetic characterisation techniques must follow the ongoing miniaturisation of devices to sizes of the order of 100 nm. The study of magnetic domain patterns is a powerful tool to analyse the local magnetic behaviour of magnetic thin films for magneto-recording and spintronics [3]. Magnetic force microscopy is a valuable technique to investigate the reversal mechanisms of the magnetisation in micrometric and sub-micrometric patterned thin films that cannot be studied with magneto-optical methods because of their limited resolution [4,5]. However, acquiring tens or hundreds of images consecutively at different applied magnetic fields is often impossible or impractical. Therefore, in this work a field-dependent MFM-derived technique is discussed and applied to sub-micrometric magnetic dots.

Materials and Methods

Square dots of $Ni_{80}Fe_{20}$ (size 800 nm and 2 µm, thickness 30 nm) have been prepared by sputtering on Si-oxide substrates and subsequently patterned by means of electron beam lithography. Experimental local hysteresis loops are obtained by repeatedly scanning the same profile of the studied patterned structure with an MFM. Each scan is performed under the application of an in-plane magnetic field having a different intensity, whose variations are synchronised with the end-of-line TTL signal of the microscope. By properly analysing the phase signal of the magnetic force microscope and plotting it as a function of the applied magnetic field, local hysteresis loops can be measured on micrometric and sub-micrometric structures [6].

Results and Conclusions

An example of magnetic domain configuration in a square dot having a size of 2 µm is shown in Figure 1 for different applied field values. The arrows schematically indicate the alignment of the magnetisation within each domain. Although in this way it is possible to follow the complete magnetisation reversal processes of the studied structure, the acquisition of tens or hundreds of images is time-consuming and often impossible because of the wearing out of the MFM tip. Therefore, a different approach is envisaged. An example of a local hysteresis loop measured on a 800 nm large $Ni_{80}Fe_{20}$ square dot is shown in Figure 2: panel (a) shows the repeated scan of a cross section of the dot, making visible the dot edges and its width. Panel (b) shows the corresponding phase signal, sensitive to the magnetic interaction between the dot and the tip, that changes as a function of the applied magnetic field, reported in panel (c). Panel (d) is a vertical cross section of panel (c), showing the correspondence between the scan line number and the applied field.

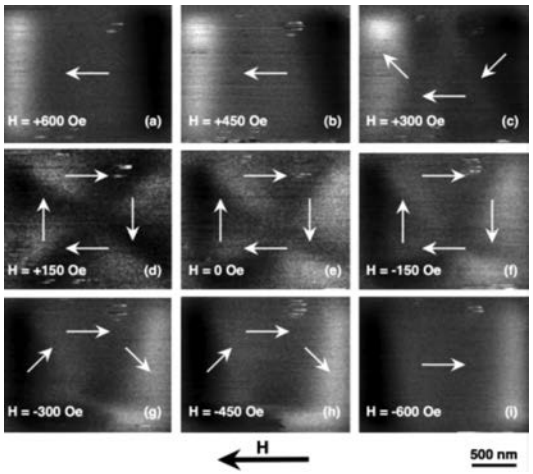

Figure 1. MFM signal (phase channel) of a $Ni_{80}Fe_{20}$ square dot with a size of 2 µm acquired at different applied field values.

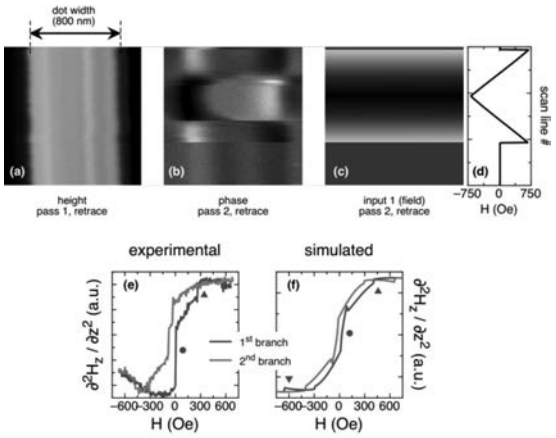

Figure 2. $Ni_{80}Fe_{20}$ dot with a size of 800 nm. (a) Height channel of the chosen profile, repeated over time. (b) Phase channel (magnetic signal). (c) Applied magnetic field value, (d) as a function of the scan line number. (e) MFM local hysteresis loop (experimental) and (f) corresponding simulated loop. Up triangles: formation of C-state; circles: nucleation of the vortex; down triangles: vortex expulsion.

By properly analysing the phase signal, for example by determining the phase contrast close to the dot left and right edges, local "hysteresis loops" can be extracted from the MFM measurements, as shown in panel (e). These loops plot the field dependence of the second derivative along *z* of the magnetic field generated by the distribution of the magnetisation of the sample, in the volume where the MFM tip is located, and represent the evolution of the magnetic domain configuration as the field is swept. Characteristic features of the magnetisation process, such as vortex nucleation and expulsion, or transition from saturation to C-state are identified. The experimental data are compared with micromagnetic simulations performed on a model system having the same composition and geometry as the studied sample. The equilibrium configuration of the magnetisation is calculated for each applied field value. Then, the map of the second derivative of the field generated by the magnetisation is computed, wich can be directly compared with experimental MFM images. Finally the same analysis procedure is applied on the calculated field maps, and the simulated "hysteresis loop", having the same meaning as the experimental one reported in Figure 2 (e), is obtained from the simulated data (Figure 2 (f)). The agreement between experimental and simulated MFM maps, at different applied fields, and "hysteresis loops" provides the necessary validation for the technique. By means of this technique, the deep investigation of the magnetisation reversal process in patterned structures can reveal insightful details concerning the magnetisation equilibrium states, thanks to the MFM high spatial resolution and the accurate control of the applied magnetic field.

References

1. H.S. Nalwa, Magnetic Nanostructures, H.S. Nalwa ed. (American Scientific). 2002
2. H. Dery, et al. Nature. 2007;447:573
3. T. Shinjo, Nanomagnetism and spintronics, (Elsevier, Oxford, UK). 2009
4. T.G. Sorop, et al. Phys Rev B. 2003:67:014402
5. R.P. Cowburn, M.E. Welland. Science. 2000:287:1466
6. M. Coïsson, et al. Phys. Rev. Appl. (submitted)

Mechanical and piezoelectric analysis of ferroelectric domains in BFO thin films

F. Dinelli,[1] C.-E. Cheng,[2,3] C.-S. Chang,[2] F. Chien,[3] Y.-C. Chen[4]

[1]*Istituto Nazionale di Ottica, CNR, Pisa, Italy*
[2]*Department of Photonics, National Chiao Tung University, Hsinchu, Taiwan*
[3]*Department of Physics, Tunghai University, Taichung, Taiwan*
[4]*Department of Physics, National Cheng Kung University, Tainan, Taiwan*

Corresponding author: F. Dinelli
E-mail: franco.dinelli@ino.it

Key words: AFM, UFM, PFM, ferroelectric, thin films.

Introduction

Recent advances in thin-film engineering have led to the realization of $BiFeO_3$ (BFO) epitaxial films, a new type of mixed-phase system driven by the substrate strain. [1] Under a strong compressive strain (>4%), the most stable crystalline structure can be transformed from the rhombohedral-like monoclinics (R) to tetragonal-like monoclinics (T). Additionally, the coexistence of R- and T-phase can be obtained in the same film with an appropriate strain relaxation through the film thickness.

This mixed-phase system can provide a template to reveal the origins of physical properties in relaxor and morphotropic phase boundary materials, such as large piezoelectric response and enhanced ferroelectric polarization. [2] In this work, we present a study of the piezoelectric and mechanical properties of T-R mixed-phase stripes by means of piezoresponse and ultrasonic force microscopies (PFM, UFM).

Materials and Methods

Our microscope is a homemade system. In particular the head is a commercial NT-MDT Smena suitable for electrical measurements; the electronics and the software used for control and acquisition are both developed in house. For both UFM and PFM, we use a function generator (Agilent 33220A) and a double lock-in amplifier (Zurich, HF2LI). The color codes of the images are the following: topography, whiter for higher regions; UFM, whiter for higher elastic moduli; PFM, whiter for larger out-of-plane response.

The tip employed is a diamond coated one (DCP11, NT-MDT). PFM [3] is generally operated at 20 kHz and 5V. UFM [4] is operated at around 4MHz with an amplitude modulation of around 1 nm at 4kHz. The two techniques can be performed in the same place, with no need to withdraw the tip. This can be simply obtained by switching the electrical connection to the top electrode of a piezo-plate located directly under the sample.

The sample herein reported is a mixed-phase $BiFeO_3$ (BFO) film with a thickness of 150 nm, grown by pulsed laser deposition on conducting $LaNiO_3$ (LNO) buffered (001) $LaAlO_3$ (LAO) substrates.

Results and Conclusions

In the Figure 1, we show some of the results obtained. The topography of flat (T-phase) and stepped regions (mixed R- and T-phase) is presented along with the PFM and UFM signals obtained. From the topography profile shown in the graph, it is possible to verify that the vertical scale of the mixed phase regions is around 1 nm, whereas the lateral dimension of the stepped regions ranges around 50 and 100 nm. Therefore, though the R-phase steps in the graph appear very steep, in reality they are quite flat.

In order to help the reader to visualize the data obtained, we have superposed stripes of UFM and PFM signals on the corresponding morphology. Starting with the PFM data, it is possible to identify the different ferroelectric domains: the whiter regions are those where it has been measured a larger out-of-plane response for a constant oscillating voltage applied.

In addition to the topography profile of a mixed-phase region, in the graph we show the corresponding UFM signal (light grey). It can be clearly seen that the regions with larger UFM signal correspond to the less steep regions, identified with the T-phase. It is thus possible to state that the R-phase regions are more compliant than the T-phase ones. This is for the first time established, according to the literature published up to now.

Finally, not reported here in details, we have also applied a DC vertical bias in order to switch the piezoelectric domains in square areas of the flat T-phase regions. PFM shows that depending on the bias amplitude partial or full inversion can be obtained. UFM indicates that the mechanical prop-

erties of the fully inverted domains do not change

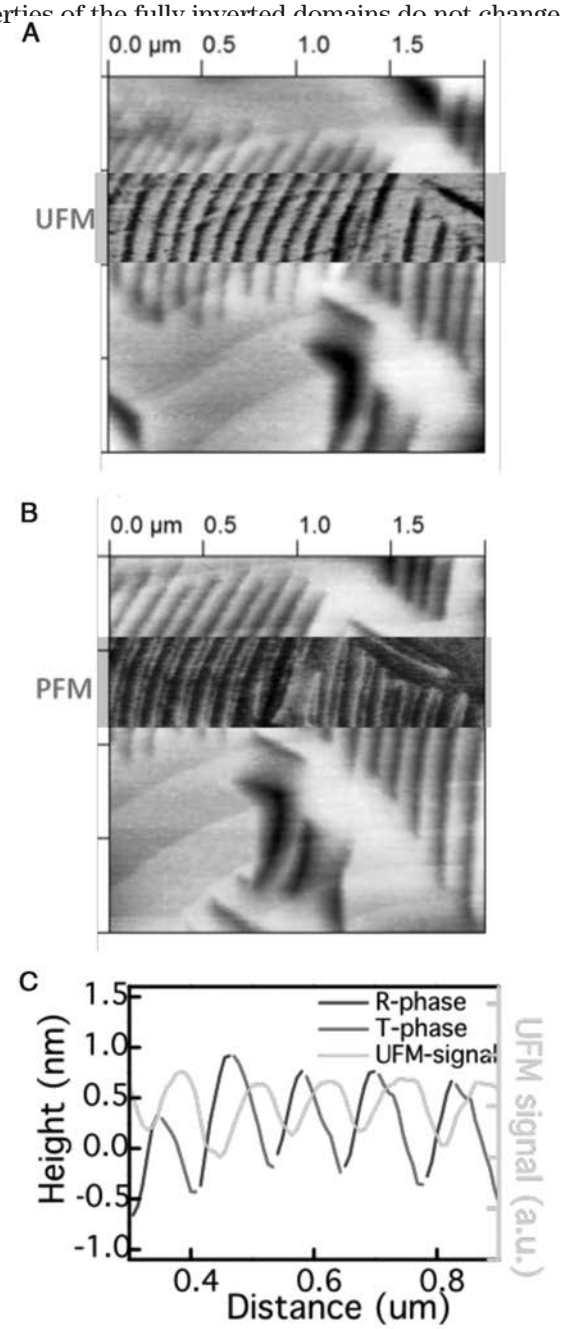

Figure 1. A. The grey-scale stripe represents the UFM signal superposed to the topography (white-black scale). B. The grey-scale stripe represents the PFM signal superposed to the topography. C. Line profiles of UFM (light grey) and topography.

Acknowledgments

Cheng-En Cheng thanks National Science Council of Taiwan and National Chiao Tung University for travelling support. All the authors thank Dr. Pasqualantonio Pingue for his help.

References

1. R. J. Zeches, et al. Science 2009;326 :977
2. Y.-C. Chen, et al. Adv. Mater. 2012;24:3070
3. A. Gruverman, J. Vacuum. Sci. Technol. B. 1995;13:1095
4. O. Kolosov, K. Yamanaka, Japan. J. Appl. Phys. Part. 2-Letters 1993;32(8A):L1095

Structure of self-assembled iron-phthalocyanines on the Au(110) surface through STM imaging and DFT calculations

S. Fortuna,[1,2*] P. Gargiani,[4] M. G. Betti,[4] C. Mariani,[4] A. Calzolari,[3] S. Fabris[1,2]

[1]*CNR-IOM DEMOCRITOS, Theory@Elettra group, S.S. 14, km 163.5, I-34149 Trieste, Italy*
[2]*SISSA, Via Bonomea 265, I-34136, Trieste, Italy*
[3]*CNR-Nano Istituto di Nanoscienze, Centro S3, I-41125 Modena, Italy*
[4]*Dipartimento di Fisica, Università di Roma La Sapienza, Roma, Italy*

Corresponding author: S. Fortuna
E-mail: sara.fortuna@uniud.it
*now at the Department of Medical and Biological Sciences, University of Udine, Italy

Key words: phthalocyanine, Au(110), self-assembly.

Introduction

STM imaging is a powerful tool to unravel the pattern formed by surface-adsorbed molecules, generally controlled by the interplay between intermolecular and molecule-substrate interactions. For instance metal-supported metal-phthalocyanines, large conjugated cross-shaped molecules capable to coordinate most of the transition metals, can self-assemble on flat metallic surfaces into ordered aggregates whose ordering details depend on the symmetry and periodicity of the substrate. For instance square and hexagonal lattices have been observed on (111) surfaces, while Kagome lattices are observed on graphene.

Highly anisotropic surfaces can act as templates for the self-assembly, as in the case of (110) surfaces of fcc metals, where organic molecules have been observed to align along the [110] direction. A special case is that of the Au(110) surface where also the propensity of the surface toward reconstruction comes into play. Indeed the metal–surface interaction between aromatic molecules and Au(110) induces the rearrangement of the naturally reconstructed 1 × 2-Au(110) surface into surfaces of different periodicities. Density functional theory calculations can reveal the energetic origins of the molecule-driven substrate reconstruction, as exemplified in our recent work on the FePC/Au(110) (full paper in Ref.[1-2]).

Results and Conclusions

The molecule-driven surface reconstruction of the FePc on Au(110) allows to understand whether and up to which extent the molecule-substrate interplay can induce a self-templating effect of the metal surface that can guide the linear self-assembly of a planar molecular system. By STM imaging (Figure 1, center), we have observed ×5 reconstructions of the clean Au(110)-1 × 2 surface in correspondence to FePc molecular chains with a regular patterning of the surface with FePc chains aligned along the reconstructed channels with each chain separated by a row of Au atoms. The diffraction patterns (Figure 1, left) confirm the 1D ordering along the channels and a ×5 periodicity along the [001] direction.

DFT calculations (Figure 1, right) predict that the periodicity along the 1D assembly is driven by intermolecular interactions. The calculated energetics show that the ×5 reconstruction formed by alternating ×2 ×3 valleys is expected to be a common surface defect due to its surface energy comparable to that of the naturally occurring ×2 reconstruction.

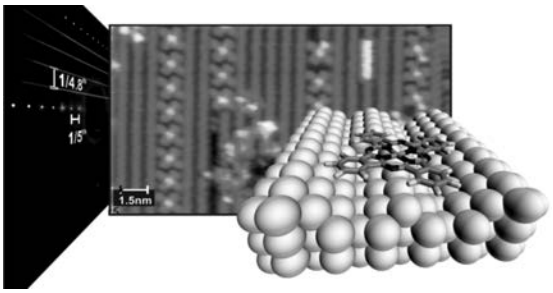

Figure 1. [left] LEED image relative to the FePc ×5 single layer with a superposition of the expected pattern obtained from STM and a theoretical surface model. The ×5 spots in the [001] direction indicate the long-range ordering of the molecular chains along this direction. The stripes stacked along the perpendicular [1100] direction are due to the absence of a definite phase among the adjacent molecular rows. [center] STM topography collected at –0.77 V and 0.4 nA in constant current mode at T = 60 K on a FePc/Au(110) at a coverage of about 0.1 SL of FePc. [right] Model of molecular adsorption and surface reconstruction resulting from the calculated energetics for the FePc/Au(110) system. The reconstruction underneath the molecule is formally obtained by the removal of two rows of Au atoms from the clean surface.

Adsorption of a FePc molecule on these ×2 ×3 line defects yields a significant binding energy, although the calculated energetics predicts that a larger molecular binding is achieved by first reorganizing the metal surface underneath the molecule in a symmetric structure.

The energy cost to reconstruct the surfaces into a more suitable template is largely compensated by the larger adsorption energy on this optimized substrate. We call this effect "self-templating". The self-templating molecule-substrate interaction process also induces a rehybridization of the electronic states localized on the central metal atom with the surface acting as a fifth ligand on the FePc metallorganic states [2].

As the electronic properties of supported organic overlayers strongly depend on the structural properties of the interface, the synergetic study of molecular-driven surface reconstructions is a key aspect in the design of novel nanodevices.

Acknowledgments

We thank the synchrotron radiation national facility ELETTRA - Sincrotrone Trieste and the Universita di Roma "La Sapienza". We acknowledge the CINECA Award N. HP10CABDLS, 2011, for the availability of high performance computing resources and support. This work was supported by the MIUR project "PRIN/COFIN" contract N. 2008525SC7 and 20087NX9Y7. In addition, the research leading to these results has received specific funding under the "Young SISSA Scientists' Research Projects" scheme 2011-2012, promoted by the International School for Advanced Studies (SISSA), Trieste, Italy.

References

1. S. Fortuna, et al. J Phys Chem C. 2012;116:6251
2. M.G.Betti, et al. J Phys Chem C. 2012;116:8657

Atomic Force Microscopy detection of antibody-antigen complexes

V. Ierardi,[1] F. Ferrera,[2] E. Millo,[2,3] G. Damonte,[2,3] G. Filaci,[2,4] U. Valbusa[1]

[1]*Nanomed lab, Physics Department, University of Genova, Via Dodecaneso,33, Genova, 16146 Italy*
[2]*Centre of Excellence for Biomedical Research, University of Genova, Viale Benedetto XV, 7, Genova, 16146 Italy*
[3]*Department of Experimental Medicine, University of Genova, Viale Benedetto XV, 1, Genova, 16132 Italy*
[4]*Department of Internal Medicine, University of Genova, Viale Benedetto XV, 6, Genova, 16146 Italy*

Corresponding author: V. Ierardi
E-mail: vincenzo.ierardi@unige.it

Key words: AFM, antibody, antigen.

Introduction

Ours idea is to use the Atomic Force Microscopy (AFM) as label-free revealing system [1]. This approach allows detecting the formation of antigen-antibody immune complexes without need of a fluorochrome labelled probe. In the process of detection of the antigen-antibody complexes by AFM the substrate functionalization method plays a central role, since the AFM is able to visualize single molecules only if the substrate roughness does not interfere with the measure.

There are several functionalization methods that allow to the antibodies to retain their orientation and/or function [2]. However, most of them are not suitable for AFM imaging, because they produce substrates presenting high roughness. Indeed, the functionalization of a suitable substrate for AFM imaging should create a monolayer of molecules that allows to the antibodies to retain their orientation and functionality without enhances the substrate roughness.

The heights of the antibodies detected by AFM varies from 4 to 6,5 nm, thus in order to permit unambiguous identification of the antibody by AFM the substrate roughness must be very low. Here a new functionalization procedure that uses a smooth solid substrate (e.g. mica, glass and silicon) and a short peptide as antibody linkers, which has a high affinity to the antibody Fc portion, is described. This procedure allows the production of surfaces with a very low roughness (below 1 nm) able to bind properly the antibodies, thus keeping their bioactivity [3, 4].

Materials and Methods

APTES-mica surface was obtained by placing the mica in a vacuum glass dessicator, which contained 50 μL of APTES 98% (Sigma-Aldrich), for 1h. To create the monolayer of antibody binding peptide on APTES-mica surface, 2 mg/mL peptide in DMF (Sigma-Aldrich) were treated with HATU and DIPEA (Sigma-Aldrich) to activate the carboxylic groups. The solution was then deposited on the APTES-mica substrate. Five solutions with different concentrations of anti-IL10 antibody (Biosource -Invitrogen, Carlsbad, CA, USA) were deposited on the treated mica solid substrate by means of a Piezoarray non-contact microarraying system (Perkin Elmer, Waltham, MA). The AFM analysis was performed using a Dimension 3100 Veeco AFM (Santa Barbara, CA, USA) with a hybrid XYZ head, using Olympus OMCL-AC160 tips with nominal apical radius <7 nm (Olympus corporate, Tokyo).

Results and Conclusions

A review of the literature has shown that particular peptides could have antibody binding activity, so we focused our attention to some small peptides, which have the ability to recognize the Fc immunoglobulin portion [5]. Using peptides sequences with high affinity for the Fc region of antibody as model system, we have identified and synthetized a new class of peptides suitable for antibodies AFM investigation. We have synthesized and tested different peptides. These peptides are able to bind with high affinity the antibody Fc portion and as antibody we have used the anti-IL10 monoclonal antibody. Indeed these peptides do not induce remarkable roughness on the substrate surface, reducing the AFM background signal, have high affinity for the antibody Fc portion and are able to link the antibody to the substrate with the proper orientation. The AFM analysis of the substrates, obtained with the peptides, shown that all of them produced surfaces with very low roughness, below 1 nm. This is due to very likely to the self-assembling peptides properties [6]. Therefore, five solutions with different concentrations of anti-IL10

antibody were deposited onto two solid supports of mica, previously coated with a layer of peptide. One support was used in order to verify the procedure by means of an immunofluorescence assay (data not shown) and the second one was used to perform AFM measurements. AFM analyses were carried on the same specimen area after the immobilization of the antibody and after the treatment with the antigen solution.

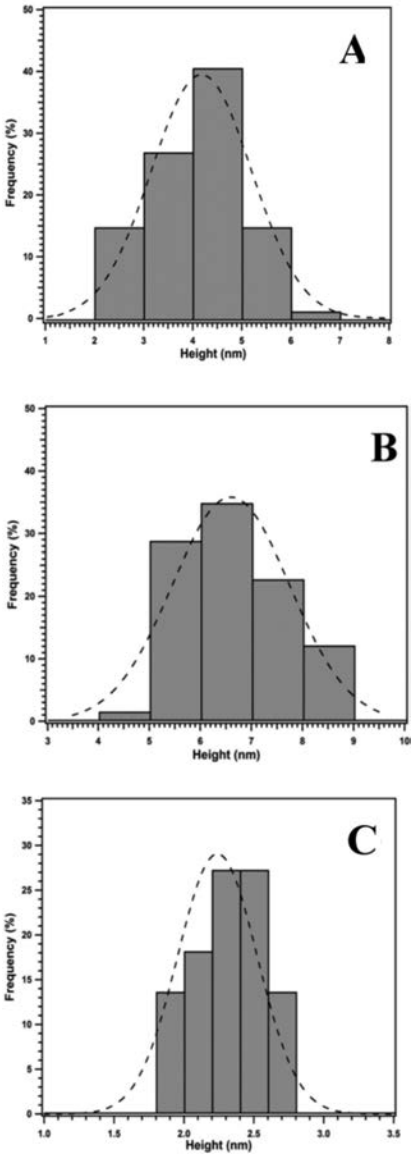

Figure 1. A) Antibody height histogram, the height of antibodies is 4.2±0.3 nm. B) Antibody-antigen complexes height histogram, the height of antibody-antigen complexes is 6.6 ± 0.3 nm C) Antigen height histogram, the height of antigens is 2.3 ± 0.1 nm.

The results of the AFM analysis are shown in Figure 1. The difference between the height of the antibody and the height of the antibody-antigen complex fits very well the height of the antigen.

In conclusion we have the proof of principle that it is possible to detect the formation of antibody-antigen complexes using the AFM as label-free technique. This result was achieved taking advantage of small peptides with a peculiar and well defined aminoacidic sequence, which confer them high affinity for antibody Fc portion. In addition we have obtained an ultra-flat surface that allows us to use the AFM as label-free detection.

References

1. M. Menotta, et al. 2010 Biosensors and Bioelectronics 25(11)
2. K Nakanishi, et al. 2008 Current Proteomics 5 161
3. V. Ierardi, et al., J.Phys.:Conf.Ser. 439, 012001, (2013)
4. V. Ierardi, et al., Patent International Publication Number: WO 2012/004721 A1, (2012)
5. G. Fassina, et al., Journal of Molecular Recognition 9 564 (1996)
6. C. Duce, et al., The journal of physical chemistry. B, 111 (5). (2007)

Quantitative AFM morphometry of non-fibrillar α-synuclein aggregation products induced by the chaperone-like protein 14-3-3η

D. Kumar,[1] N. Plotegher,[2] L. Bubacco,[2] M. Brucale[3]

[1]*Department of Biochemistry, University of Bologna, Via Irnerio 48 – 40126 Bologna, Italy*
[2]*Department of Biology, University of Padova, Viale G. Colombo 3 – 35131 Padova, Italy*
[3]*ISMN – CNR, Area della Ricerca Roma1, Via Salaria km 29.3 – 00015 Monterotondo, Italy*

Corresponding author: M. Brucale
E-mail: marco.brucale@ismn.cnr.it

Key words: Alpha-Synuclein, amyloidogenesis, morphometry.

Introduction

Idiopathic and familial forms of Parkinson's disease (PD) are associated with the abnormal neuronal accumulation of α synuclein (aS) leading to the formation of β-sheet-rich aggregates called Lewy Bodies (LBs). A connection between PD and the 14-3-3 chaperone like protein family was recently proposed, based on the fact that several 14-3-3 isoforms interact with PD-associated proteins such as parkin, LRRK2 and aS [1]. Moreover, 14-3-3 proteins show structural similarity with aS [2] and were found to be components of LBs in human PD [3]. The 14-3-3η (Eta) isoform in particular has been found associated with aS in parkinsonian brains, but not in healthy ones. In spite of the above, literature regarding the Eta/aS interplay is sparse.

Recent results [4] demonstrate that while Eta is unable to bind monomeric aS, it strongly interacts with oligomeric aS aggregates occurring during the pathological early aggregation stages of aS amyloidogenesis, drastically diverting the aggregation process even when present in sub stoichiometric amounts relative to aS.

Herein, we characterize the alternative aS non-fibrillar products (NFPs) induced by Eta via atomic force microscopy (AFM) imaging, then perform quantitative morphometry on a large pool of images to infer information about the mechanism of interaction between aS and Eta.

Materials and Methods

Protein expression and purification: aS and Eta were expressed and purified as described elsewhere [4].

Aggregation assays: Prior to aggregation, monomeric aS solutions were ultra filtered with a 100 kDa cut-off Vivaspin (Sartorius) filter to remove oligomeric aggregates. Eta was added to the aggregation mixtures to afford specific Eta:aS stoichiometric ratios of 1:4, 1:7, 1:12, 1:20, 1:24, 1:30, and 0. All aggregation experiments were carried out at 37°C in PBS supplemented with 0.05% (w/v) Sodium Azide and 5 mM DTT (when not stated differently), and providing a constant agitation at 1000 rpm. The sample volume was 200 μL and the reaction vessel a PCR vial.

Atomic force microscopy imaging was performed in PeakForce tapping mode with Scanasyst-Air probes (Bruker, Mannheim, Germany) on a Nanoscope V system equipped with a Multimode head and a type E piezoelectric scanner (Bruker, Mannheim, Germany). 10 μl of sample were deposited on freshly cleaved mica (RubyRed Mica Sheets, Electron Microscopy Sciences, Fort Washington, USA) and left to adsorb for 5 min at room temperature (~20 °C). The mica surface was then rinsed with ~500 μL of MilliQ H_2O (Millipore Simplicity) at the same temperature and dried with dry nitrogen. In most experiments, the sample was diluted ~10 times with PBS then equilibrated at RT for 10' prior to deposition in an attempt to minimize overlap of individual aS aggregates on the surface.

Results and Conclusions

While all aggregation experiments resulted in the formation of aS amyloid aggregates (Figure 1A, left column), only those obtained at an aS/Eta molar ratio of 30 or above revealed the canonical characteristics of mature aS fibrils. Fibril diameter distributions were converted into fibril section area per unit length (Figure 1A, right column). The integral of the equivalent disc area distribution calculated in the 0-75 nm^2 (and 75-300 nm^2) interval was used as an estimation of the total volume of NFPs (and fibrillar products) to generate the plot shown in Figure 1B. Our assumption is that the packing density of monomeric aS included into all aggregates is the same, thus the volumes calculated as described above are directly proportional with the amount of monomeric aS converted into the relevant aggregate type. The plots were fitted with a Langmuir isotherm (R^2=0.99) resulting in a reduced affinity constant (rK_d) of 26.6 aS

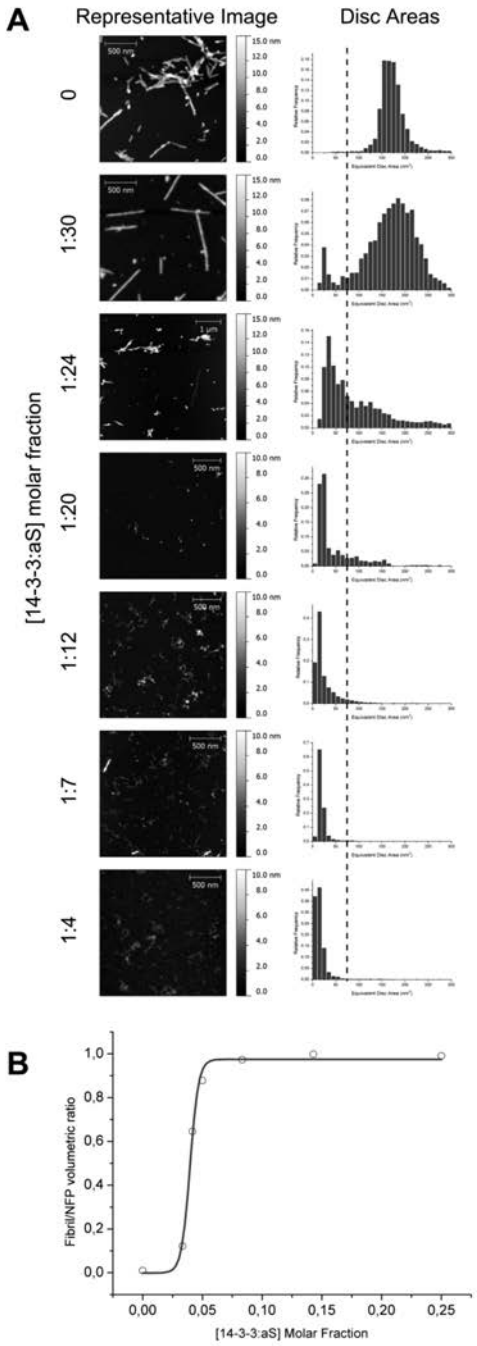

Figure 1. (A) AFM representative images (left column) and equivalent disc area distributions (right column) of the aS-NFPs induced by Eta at various relative stoichiometries. (B) Plot of relative molar fraction of starting monomeric aS trapped into NFPs (circles) VS [Eta:aS] molar ratios. The corresponding Langmuir isotherm fit is shown as a solid grey line.

equivalents per Eta homodimer. The fact that the dose-dependent repartition of monomeric aS between fibrils and NFPs can be fitted by a Langmuir isotherm showing almost no deviation from ideal behavior strongly suggests that the binding partner of Eta during aS aggregation is a specific, relatively homogeneous class of "critical" early oligomeric aggregates.

References

1. R.J. Nichols, et al. Biochem J. 2010;430:393
2. N. Ostrerova, et al. J Neurosci. 1999;19:5782
3. T. Umahara, et al. Geriatr Gerontol Int. 2012;12:586
4. N. Plotegher, et al. Manuscript in preparation

Custom system for single molecule force spectroscopy

E. Landini,[1] S. Raccosta,[2] F. D'Anca,[2] M. Zora,[3] S. Mazzola,[3] P.L. Sanbiagio,[2] V. Martorana,[2] M. Vassalli[1]

[1]*Istituto di Biofisica del CNR, via De Marini 6, Genova, Italy*
[2]*Istituto di Biofisica del CNR, Via Ugo La Malfa 153, Palermo, Italy*
[3]*Istituto per le applicazioni marino-costiere del CNR, ex Tonnara Campo di Granitola, Trapani, Italy*

Corresponding author: E. Landini
E-mail: ettore.landini@ge.ibf.cnr.it

Key words: single molecule, force spectroscopy, Atomic Force Microscopy.

Introduction

Atomic Force Microscopy (AFM) is nowadays a widely distributed imaging technique, able to achieve nanometric resolution on a broad range of samples, from innovative materials to living biological systems. The physical principle underlying the AFM technology is based on the measurement of the interaction force between a sharp tip and the sample, with picoNewton sensitivity. This aspect of AFM was more recently exploited to perform force spectroscopy experiments on single molecules, paving the way for the study of mechanical properties of single proteins and peptides [1].

This type of measurement has two major requirements: great stability and precision in terms of vertical displacement and force sensing, and the ability to acquire a large, statistically relevant, set of repeated measurements.

Apart from the stability and precision point, with commercial systems it is not always easy to gather the needed amount of curves for the analysis, since this ideally requires the instrument to be able to perform multiple curves on a number of different spots on the sample surface. To overcome this limitation, researchers have to customize their instruments and/or the control software that comes with them, spending time and also money on already expensive systems.

By tailoring the hardware and using an open source software architecture that could allow easy and fast modifications and also a complete redesign of the control software, we managed to create a system that addresses the problem cited above, without losses on the performance side.

Materials and Methods

The system consists of the following parts: a custom AFM head, with a single axis (Z) piezoelectric actuator; two piezoelectric step motors for XY movements, connected to the client PC via a USB controller; a PC running Ubuntu 10.04 with a real-time kernel patch; a National Instruments data acquisition board (NI PCI-6259), on the Linux PC to communicate with the AFM; a Windows 7 PC with .Net 4.5 for the client software.

On the software side we used an already existing open source architecture developed as part of a project called RTAI-XML [2]. The main advantage of this architecture is the separation between the hardware interface and the user one. This allows to implement both interfaces focusing on their specific features without any constraint or bond between them.

While the hardware interface and the communication server, which exchange information between the instrument and the user, run on a modified Linux pc, the client software has been developed for Windows. The reason behind this choice is that Windows is the most widely spread OS in the world and so the majority of the users won't have to get familiar with an unknown environment.

To test the performances of the system, we performed a series of experiments on the bond strength between streptavidin and biotin.

For these tests, we functionalized the cantilever chip (MSNL-10 Bruker) with streptavidin and adsorbed biotin-BSA on a borosilicate glass slide following the procedure described by Lo et al. [4], adding a further UV irradiation for both the chip and the slide for ensuring the exposure of the OH groups.

Results and Conclusions

The various tests conducted on the stability and the performances of the system showed us that, apart from the obvious tunings and improvements that characterize every prototype, the system possesses all of the characteristics that we had fixed as our objective.

The software provides all the features needed to perform experiments and allows for easy and fast modifications when needed.

On the hardware side, we managed to satisfy the key features required by the measurements in terms of stability and precision. The curve report-

ed in Figure 1A is a good example of the system performances.

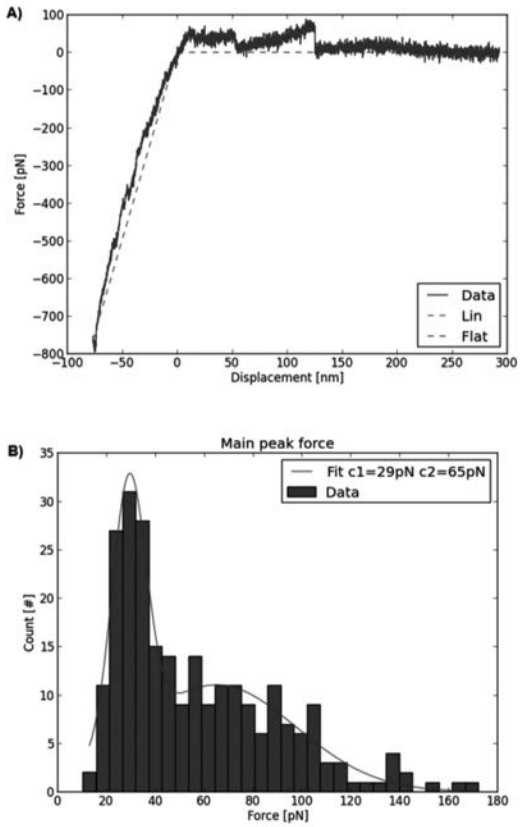

Figure 1. A) Streptavidin *vs* biotin sample FD curve; B) Main peak force histogram fitted with a sum of two Gaussian functions

Regarding the ability of gathering a large amount of curves for the sake of statistical analysis, the histogram shown in Figure 1.B has a trend that can be fitted with the sum of two Gaussian functions. The first peak is associated to non specific interaction events occurring near the contact point, at lower forces.. The second one contains the relevant information about the system under investigation: the force peak corresponds to the rupture of the bond between the streptavidin on the tip and the biotin on the glass substrate. This result shows how the remarkable quantity of curves that can be taken by the system for each experiment provides a stable statistics and as such a reliable way to distinguish positive results from the ones to be discarded, without any complex data filtering.

References

1. H. Clausen-Schaumann, et al. Curr Opin Chem Biol. 2000;4:524
2. M. Basso, et al. Proceedings of the 44th IEEE Conference on Decision and Control. 2005;2733
3. P. Mantegazza, et al. Linux J. 2000; 2000, 72es, Article 10
4. Y.S. Lo, et al. Langmuir. 1999;15:1372

Electronic characterization of bulk hetero-junctions by Kelvin Probe Force Microscopies

A. Liscio

Istituto per la Sintesi Organica e la Fotoreattività-CNR, via Gobetti 101, 40129 Bologna, Italy

Corresponding author: A. Liscio
E-mail: andrea.liscio@isof.cnr.it

Key words: Scanning Probe Microscopy, Organic solar cells.

Introduction

In this article we highlight few recent works performed making use of KPFM [1] with the aim of getting fundamental information on the nanoscale electrical and electronic properties of organic and supramolecular materials effectively employed for real opto-electronic devices, and to correlate them with their behavior on a macroscopic scale [2]. After a brief description of the scanning probe technique, this article describes the electrical nanoscale characterization of organic bulk hetero-junctions for solar cells when tested under an additional stimulus, *i.e.* light.

Technique

KPFM can be considered being modes of Atomic Force Microscopy (AFM) since it is typically operating on the very same setup. A microfabricated cantilever exposing at its edge a metal-coated tip is used to sense the surface and to map both its morphology and its electrical features. By sensing electrical signal, the tip passes over the surface but never being in direct contact with it. KPFM measures the surface potential (SP) of the sample by recording the electrostatic forces resulting from the interaction between tip and sample. KPFM is in fact a non-contact technique based on Zeeman vibrating capacitor set-up; the two electrodes of the capacitor are the sample and an oscillating tip (with defined frequency ω) rastering the surface at fixed tip-sample distance.[3] A direct quantification of the surface potential is not trivial, being the force proportional to the gradient of the tip-sample capacitance and the square of electrical potential difference between tip and sample: $F_\omega = \partial_{\omega z} C \times \Delta V^2$. This problem is circumvented by applying an adjustable bias offset between tip and sample (i.e. $F_\omega \propto SP - V_{bias}$); the resulting electrostatic force is detected by a lock-in amplifier, and a feedback circuit controls the applied bias until the surface potential is compensated. This provides a direct quantification of the surface potential corresponding to the applied bias to stop the tip oscillations. The physical meaning of the measured SP is strictly related to the sample electrical properties. In the case of metallic samples, the measured surface potential corresponds to the work function difference between tip and sample. Moving from metallic to semiconducting or even insulating samples, SP is not directly correlated to the work function anymore, but is instead influenced by local charge density [4].

Results and Conclusions

In a bulk hetero-junction the morphology and the electronic properties of the blended material are key factors for the device efficiency and performance. In particular, the morphology plays a paramount role in the percolation pathways for transport of both photogenerated excitons and charges. KPFM measurements can correlate on the nanoscale the morphological properties with photogenerated charges, and it allows to monitor dynamical production, transport and recombination of charges. Bulk hetero-junctions are phase-segregated films obtained by co-deposition of an electron-donor and an electron-acceptor on a surface. The connectivity and percolation of both the electron- and hole-transporting phases with their respective electrodes represent the key-factor for efficient organic solar cells. Hoppe *et al.*[5] studied on solid-state blends of poly[2-methoxy-5-(3,7-dimethyloctyloxy)]-1,4-phenylenevinylene (MDMO-PPV) and the soluble fullerene C60 derivative 1-(3-methoxycarbonyl) propyl-1-phenyl [6,6]C61 (PCBM), spin-cast from either toluene or chlorobenzene solutions. KPFM revealed distinct differences in the energetics on the surface of films cast from two solvents; by gathering complementary information by scanning electron microscopy, it was concluded that the films prepared from toluene solutions do not exhibit percolation pathways for electrons propagation toward the cathode. Authors also suggest that the reduced performance of devices with coarse phase separation is at least partially due to a limited electron transport within the film. The direct observation of the contact region between donor-acceptor material that results to be the only "light active" has been shown by Liscio *et al.*[6] through KPFM

analysis of $CHCl_3$ cast N,N"-bis(1-ethylpropyl)-3,4:9,10-perylenebis(dicarboximide) (PDI) and regioregular poly(3-hexylthiophene) (P3HT) blends. It was proved that only the PDI clusters that are in physical contact with P3HT exhibit an appreciable charge transfer because of the existence of a complementary electron donor phase. Upon illumination with white light, the surface potential of the P3HT phase became more positive and showed a value close to that of the substrate while PDI clusters in contact with P3HT became more negative (Figure 1).

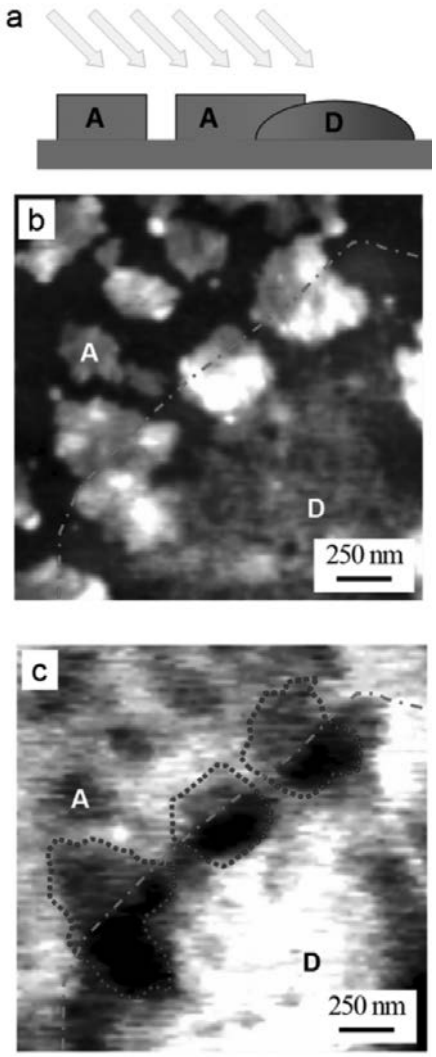

Figure 1. (a) Cartoon showing (A) PDI nanocrystals in contact or not with (D) P3HT aggregates. b) AFM and c) KPFM image recorded under illumination. Only the part PDI clusters physically in contact with P3HT are involved in the photo-charge generation. Z-range: (b) 30 nm and (c) 90 mV.

The measured potential variation induced by the light corresponds to a photo-induced charge density amounting to about 10^3 charges/mm^2. In general, one of the reasons of the success of KPFM as a powerful tool to explore bulk heterojunctions is given by its bulk sensitivity. Cadena *et al.*[7] directly showed the sub-surface sensitive of KPFM by imaging networks of single-walled nanotubes dipped into a polyimide matrix. By devising a 3D model to single out the surface and the bulk contributions to the measured potential signal, Liscio *et al.*[8] described the sampling depth in terms of film electrical permittivity, showing that on P3HT films the sub-surface sensitive of the technique amounts to about 100 nm.

Acknowledgments

Thanks are due to Emanuele Treossi, Vincenzo Palermo and Paolo Samorì.

References

1. M. Nonnenmacher, et al. Appl Phys Lett. 1991;58:2921
2. C. J. Brabec, et al. Chem Soc Rev. 2011;40:1185
3. A. Liscio, et al. Acc Chem Res. 2010;43:541
4. Y. X. Shen, et al. Rev Sci Instr. 2008;79:096106
5. H. Hoppe, et al. Adv Funct Mater. 2004;14:1005
6. A. Liscio, et al. J Am Chem Soc. 2008;130:780
7. M. J. M. Cadena, et al. Nanotech. 2013;24:135706
8. A. Liscio, et al. Small. 2011;7:634

Electrical properties of silicon nanodots embedded in a SiC matrix for photovoltaic applications

M. Perani,[1] D. Cavalcoli,[1] M. Canino,[2]
M. Allegrezza,[2] M. Bellettato,[2] C. Summonte[2]

[1]Department of Physics and Astronomy, University of Bologna, viale B. Pichat 6/2, 40127 Bologna, Italy
[2]CNR-IMM, via Gobetti, 101, 40129 Bologna, Italy

Corresponding author: M. Perani
E-mail: martina.perani2@unibo.it

Key words: AFM, Photovoltaic, Si nanodots.

Introduction

Efficiency increasing and cost reduction are key concepts in the development of the photovoltaic field and one of the factors responsible for power loss in single bandgap solar cells is that, for photons with energy higher than the band gap, the excess energy is lost by thermalization. One way to overcome this limit is to introduce the multi-junction concept, where the device has more than one bandgap [1]. In this framework, silicon nanocrystals (Si NCs) embedded in a dielectric matrix were proposed as absorbers in all-Si multi-junction solar cells thanks to the quantum confinement capability of the Si NCs, that allows a better match with the solar spectrum [2,3]. SiC as a dielectric matrix is considered promising thanks to its better conduction properties and lower barrier to the Si NCs with respect to e.g. SiO_2 [1].

Current-Atomic Force Microscopy (c-AFM) is widely used to determine the local electrical properties of semiconducting thin films at the nanoscale [4]. A conductive probe is put in contact with the surface and the current flowing between the tip and the sample is measured at constant bias [4]. In the present contribution c-AFM has been used to characterize features related to Si NC clusters in SiC on a local scale, giving a fundamental insight on their properties at microscopical level.

Materials and Methods

Silicon Rich Carbide (SRC)/SiC multi-layers are deposited by Plasma Enhanced Chemical Vapor Deposition on quartz. The precursor gases used are SiH_4, CH_4 and H_2, the temperature of the substrate is 325°C. The multi-layers are composed by a stack of 30 bi-layers of SRC and SiC. The silicon fraction in the SRC layers is 0.85. The thickness of the as-deposited layers is 9 nm for SiC and varies between 2 and 4 nm for SRC. A sacrificial a-Si:H layer (20 nm thick) is deposited on top of the shallowest SiC layer in order to prevent SiC surface oxidation during the subsequent annealing for Si NC formation [5], which is performed at 1100°C for 30 minutes. A wet etching is performed subsequently in order to remove the sacrificial layer [6]. Parallel Ni contacts are evaporated for current-voltage measurements. A dry etching (SF_6+0_2, 20 s) is used to remove the shallowest SiC layer from the surface before local conductivity measurements.

AFM (NT-MDT Solver P47H Pro microscope) is performed in contact mode to measure the surface topography and the local conductivity. The probe used is a conductive, Pt coated tip, with nominal radius of curvature of 35 nm.

Results and Conclusions

Current-AFM is the technique used to measure the local conductivity of the sample to identify the current paths at the nanoscale. A 1x1 μm^2 map taken on the sample with SRC layer thickness of 4 nm is shown in Figure 1.a. The bias applied to the tip is +2 V and the current ranges between 0 and 100 pA. The darker areas in the image correspond to higher conductivity. Regions with different conductivity can be noted. These regions are not directly correlated with some topographical features, therefore morphology-related artifacts can be excluded. Similar behaviors observed for the samples with different SRC layer thickness. Considering that in this material different phases (amorphous and crystalline) and compositions (SiC and Si) coexist, the differences in the local conductivity can be related to phase or compositional variations. Moreover, the role of impurities and/or to unintentional doping by contamination with N and O could be envisaged. The map shows cluster (likely related to Si or SiC NCs) with different conductivities embedded in a quite uniform matrix. We could attribute the different conductivity of the clusters to compositional variation (Si content) and/or impurity contamination, as also observed in nc-Si:H [7].

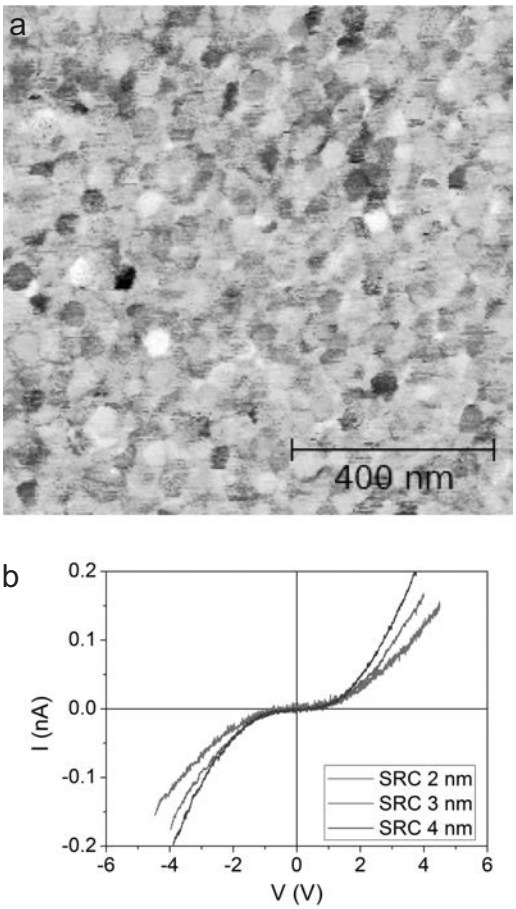

Figure 1. (a) C-AFM performed on sample with SRC layer thickness of 4 nm. (b) Local IV measured with AFM for different SRC layer thickness. Each curve is the average of 10 measurements taken in different positions on the sample surface.

IV characteristics have been measured locally with AFM in contact mode. The curves are shown in Figure 1.b and show a defined trend: at the same bias the current increases with increasing SRC layer thickness. It is possible to compare this result with the lateral conductivities measured with the deposited Ni contacts. The conductivity increases from $9.3 \cdot 10^{-6}$ S/cm to $1.7 \cdot 10^{-5}$ S/cm with increasing SRC layer thickness (2-4 nm), showing the same trend of the local measurements [8].

c-AFM is used to characterize the electrical properties of the multi-layers, showing variations at the nanoscale in the conductivity. Local IV measurements show a defined trend with SRC layer thickness, in agreement with what is observed for the lateral conductivity.

Acknowledgments

This research has been supported by the EU (FP7) under Project No.n° 245977 (NASCEnT). Martina Perani gratefully acknowledges the Spinner 2013 project of Emilia-Romagna Region for the financial support of her PhD scholarship.

References

1. G. Conibeer, et al. Thin Solid Films. 2006;511-512:654; Thin Solid Films. 2008;516:6748
2. Z. Wan, et al. Nanoscale Res Lett. 2011;6:129
3. M. A. Green, Mat Sci Eng B-Solid. 2000;74:118
4. C. Teichert, I. Beinik, in "Scanning Probe Microscopy in Nanoscience and Nanotechnology 2", B. Bhushan ed. (Springer, Berlin). 2011, 691
5. M. Zacharias, et al. Appl Phys Lett. 2002;80:661
6. M. Canino, et al. Mat Sci Eng B. 2013:178:623
7. D. Cavalcoli, at al. Nanotechnology. 2010;21: 045702
8. M. Schnabel, et al. to be presented at MRS Spring Meeting 2014 Symposium A

Interfacial properties of ionic liquids investigated by atomic force microscopy

A. Podestà, M. Galluzzi, S. Bovio, P. Milani

CIMaINa e Dipartimento di Fisica, Università degli Studi di Milano, via Celoria 16, 20133 Milano, Italy

Corresponding author: A. Podestà
E-mail: alessandro.podesta@mi.infn.it

Key words: atomic force microscopy, ionic liquids, interfacial properties.

Introduction

Beside their industrial applications, where their bulk physico-chemical properties are relevant, room-temperature ionic liquids (ILs) can also be used as electrolytes in several devices aimed at conversion and storage of energy, such as electrochemical supercapacitors, Grätzel solar cells and batteries, as well as lubricants in micro electromechanical devices. In these devices ILs are in form of thin films, or they can be spatially confined in nanoscale pores, therefore a key role is played by their interfacial, rather than bulk, properties, specifically pertaining to the solid-liquid interface. In particular, structural-morphological and electrical properties of the first few nanometers of ILs interacting with surfaces of solid electrodes are expected to have the strongest impact on device performance.

Here we report on the characterization of interfacial properties of [Bmim][NTf2] supported on different solid silica and mica surfaces carried out primarily by advanced atomic force microscopy (AFM) techniques.

Results and Conclusions

Thin films of prototypical ILs have been studied on a variety of surfaces of applied relevance, characterized by different surface chemistry (silica, mica and graphite), and different surface morphology (mica, graphite and crystalline silica are almost atomically smooth; amorphous silica has roughness below 1 nm). [Bmim][ntf2], an imidazolium-based IL, has been used because it is widely employed in applications and it is also very resistant to moisture as well as chemically and thermally stable.

The following scientific tasks have been successfully accomplished:

1. Development of suitable protocols for the deposition of nanometer-thick IL layers on selected surfaces;
2. Morphological, structural and mechanical characterization of supported IL films;
3. Characterization of the dielectric properties of supported IL films;

Figure 1 shows a remarkable example of structural reorganization of [bmim][ntf2] deposited on silica by drop-coating, i.e. by spotting a droplet of very diluted IL/methanol solution onto the surface and waiting for solvent evaporation. Topographic maps suggest that in the presence of a (charged) surface, the IL self-assembles in vertically ordered, layered structures, whose heights can easily exceed 50 nm [1-3]. Using different solvents (methanol, chloroform) and by means of X-ray photoemission spectroscopy analysis, we could rule out the hypothesis that this structural organization is the result of the complexation of IL with the solvent. The statistical analysis of AFM topographies maps provided an accurate characterization of the basic molecular step of layered structures, d~0.6 nm, consistent with the size of the cation/anion pair. Remarkably, we measured the same values of the basic step when using different solvents, on all different surfaces (excluded graphite, where extended solid-like domains where not observed). Direct nanomechanical tests confirmed the high mechanical resistance of these structures to vertical loads [2,3]; moreover, upon application of high lateral stresses, the structures presented delamination similarly to lamellar solids [2,3]. Indentation patterns of AFM tip on solid-like IL domains have been directly observed in nanomechanical tests [4], with rupture forces much higher than those reported for solvation layers at the bulk liquid/solid interface by Atkin *et al.* [5].

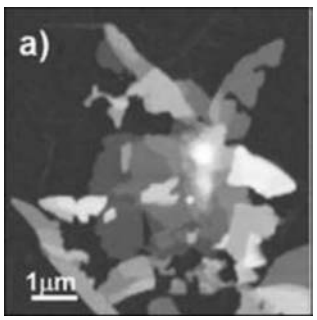

Figure 1. Layered [bmim][ntf2] island on silica.

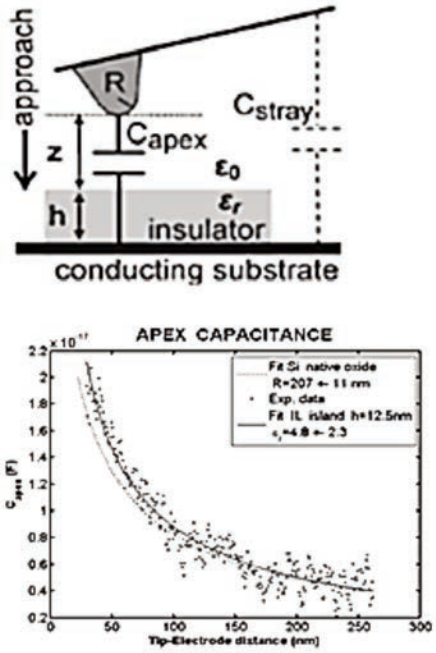

Figure 2. Capacitance vs. Distance spectroscopy on solid-like IL islands.

The observation that supported ILs islands were not disrupted by intense electric fields up to 10^8-10^9 V/m (obtained biasing the AFM with respect to sample during imaging) further confirmed that ions are tightly bound in a solid-like structure. Current-sensing AFM was used to test the dielectric properties of solid-like ILs islands, in particular to verify that, similarly to standard solid crystalline salts, also ILs islands possess dielectric character, with a finite dielectric constant (Figure 2). A static dielectric constant ε_r=3-5 was measured [6], to be compared with higher dielectric constant measured in bulk liquid ILs ε_r=9-13 [7,8].

The interest of our results motivated a sizeable computational effort, primarily represented by the activity of the Belfast and Milano groups, working in close collaboration with our team. Simulation results confirmed the layering of the IL at the interface, with a periodicity that closely matches the experimental one [3]. Moreover, simulations have reproduced semi-quantitatively the indentation patterns observed in AFM experiments [4]. Further simulations and experimental work is needed to fill the residual gap still separating the computational and experimental picture.

Acknowledgments

Thanks are due to M. Sampietro, G. Ferrari and collaborators for providing dedicated front-end electronics for AFM measurements; thanks to Cristina Lenardi, Pietro Ballone, Mario del Pópolo and Nicola Manini for fruitful collaboration along the past years.

References

1. S. Bovio, et al. J Phys Chem B. 2009;113:6600
2. S. Bovio, et al. ACS Symposium Series 2009;1030(Chapt 19):273
3. S. Bovio, et al. J Phys: Condens Matter. 2009;21:424118
4. P. Ballone, et al. Phys Chem Chem Phys. 2012;14:2475
5. R. Atkin, et al. J Phys Chem C. 2007;111:5162
6. M. Galluzzi, et al. in preparation
7. Singh, et al. J Phys Chem B. 2008;112:12968
8. H.Z. Weingartner. Phys Chem. 2006;220:1395

Combined topographic/mechanical colloidal probe imaging for the investigation of cellular interactions

L. Puricelli, M. Galluzzi, C. Schulte, P. Milani, A. Podestà

CIMaINa e Dipartimento di Fisica, Università degli Studi di Milano, via Celoria 16, 20133 Milano, Italy

Corresponding authors:
L. Puricelli
E-mail: luca.puricelli@unimi.it
A. Podestà
E-mail: alessandro.podesta@mi.infn.it

Key words: AFM, nanomechanics, living cells, finite thickness effect, colloidal probes.

Introduction

In the last two decades AFM has proved to possess a great potential in the biomedical and regenerative medicine fields as a tool to characterize mechanical and morphological properties of living cells, which were shown to be correlated to the cells' patho-physiological state [1]. Despite the wealth of experimental and technical informations provided by the reports published so far, a robust and commonly accepted methodology, regarding all the steps of the experimental activity, is still missing; this represents an obstacle to the effective exploitation of AFM-based nanomechanical approaches as biomedical tools. We have addressed some major *open issues* in AFM nanomechanics applied to living cells, such as the choice of the best AFM probe and the effect induced by the finite thickness of the cellular specimen on the measured Young modulus (*finite thickness effect*). The proposed solutions have been implemented in a protocol based on the use of micrometer-sized spherical probes for the combined topographic and mechanical imaging of living cells. An example of application of the protocol, regarding the correction for the finite thickness effect, is reported and briefly discussed.

Materials and Methods

Despite the fact that commercial sharp AFM tips have been so far widely employed in the field of cells' nanomechanics, several questions have been raised about the reliability of the mechanical properties measured on such soft and fragile samples using these probes. The critical points can be summarized as follows:

1) The small radii of curvature of commercial AFM tips (typically a few tens of nm) imply the application of high pressures and strains to the cells' surface, potentially leading to the damage of their outer membrane or the underlying cytoskeleton [2];
2) Commercial tips can show significant deviations from the ideal geometrical shape described by the corresponding contact mechanics model, thus introducing a significant source of error in the global statistics;
3) Cells are characterized by a strong structural heterogeneity and dynamical activity at the nanoscale, which could result in large standard deviations in the collected statistics [2,3].

A practical alternative to the commercial AFM tips is represented by spherical *micrometric* probes, also called *colloidal probes*. Their main advantages can be summarized as follows:

1) The applied force can be spread on a much wider area, thus significantly reducing pressures and the risk of cells' damaging;
2) They can be reliably produced and accurately characterized directly in the laboratories, according to an established characterization protocol [4];
3) They smear out nanoscale inhomogeneities, providing mesoscopic robust values of the Young modulus [2,3].

In addition, Dimitriadis and coworkers [2] developed an analytic approximate correction, for the case of spherical probes, to take into account the aforementioned finite thickness effect. This allowed us to characterize mechanical properties also of the thinnest cells' peripheral regions (cytoplasmic protrusions), whose importance is justified by their role in cells' motility and richness in focal adhesions. Here we report on the validation of our topographic/mechanical imaging protocol and of the finite thickness correction procedure, tested on living cells, cultured *in vitro* and then transferred into a custom thermostatic AFM fluid cell (@37°C).

Results and Conclusions

In Figure 1 topographic and mechanical maps acquired on a cell from the line PC12 (pheochromocytoma of the rat adrenal medulla) are shown; maps were acquired by means of a colloidal probe with radius $R \approx 5$ μm. Cells appear more rigid because of their finite thickness and the presence of a rigid substrate underneath.

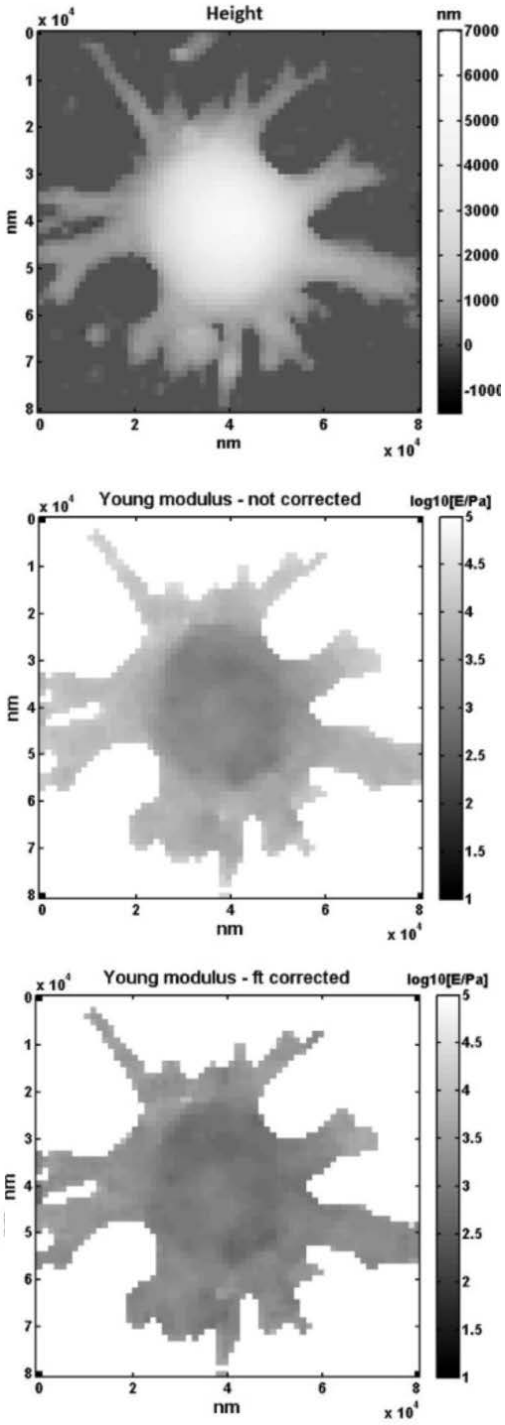

Figure 1. 2D AFM maps of a PC12 cell: height (top), uncorrected Young modulus (center), finite-thickness corrected Young modulus (bottom).

A quantitative comparison between Young moduli with or without finite thickness correction is shown in Figure 2 by means of histograms; when the correction is applied, we notice an overall decrease of the cell's Young modulus, and a relative decrease of the rigidity of the thinner cellular extensions with respect to the higher cell body, according to expectations (the two different contributions are strongly convolved).

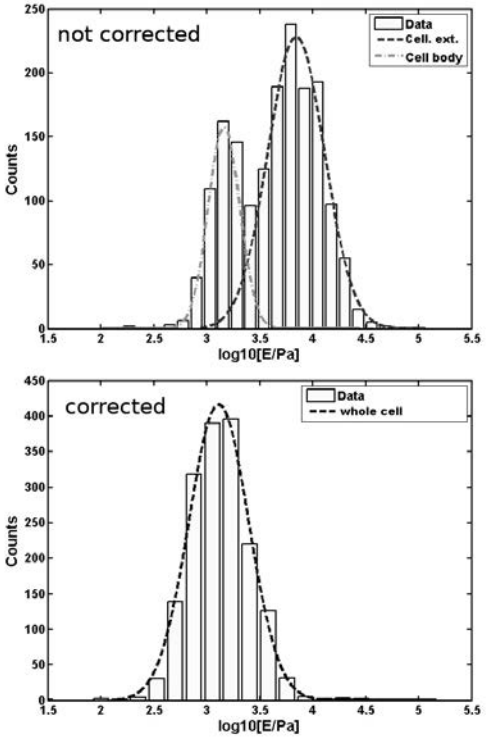

Figure 2. Histograms of Young moduli from maps shown in Figure 1: uncorrected Young modulus (top), finite-thickness corrected Young modulus (bottom).

Acknowledgments

Thanks are due to C. Lenardi for support in the cell culture lab; to R. Simonetta, M. Indrieri, D. Piotti and F. Fanalista for help in AFM measurements.

References

1. M. Plodinec, et al. Nat Nanotechnol. 2012;7:757
2. E. K. Dimitriadis, et al. Biophys J. 2002;82:2798
3. P. Carl, H. Schillers. Pflug Arch Eur J Phy. 2008;457:551
4. M. Indrieri, et al. Rev Sci Instrum. 2011;82: 023708

Analysis of the conformational space of murine prion protein: an amyloidogenic protein involved in neurodegenerative disorders

A. Raspadori,[1] V. Vignali,[2] G. Zuccheri,[2] B. Samorì,[2] G. Legname[1]

[1]*Laboratory of Prion Biology, International School for Advanced Studies, via Bonomea 265, Trieste, Italy.*
[2]*Laboratory of Nanobiotechnology, Department of Pharmacy and Biotechnologies, University of Bologna, via San Giacomo 11, Bologna, Italy*

Corresponding author: G. Legname
E-mail: legname@sissa.it

Key words: prion protein, conformational space, aggregation, force spectroscopy.

Introduction

Protein folding involves a stochastic search through the configurational energy landscape of the protein to find the native structure. Although most proteins have evolved to fold efficiently into a unique native structure, misfolding (the formation of non-native structures) occurs frequently *in vivo*. Biophysical studies of protein misfolding and early stage aggregation processes are very complex due to the presence of many conformations and different misfolding routes. Single-molecule approaches have proven to be good methods to evaluate the conformational heterogeneity of biological macromolecules, because they can discern amongst different subpopulations, rare or transient states and their energy barriers.

The cellular form of the prion protein (PrP^{C}) is a highly conserved membrane-bound protein that is able to misfold into an infectious conformation (PrP^{Sc}), which can form aggregates and fibrils with different biochemical and biological properties. Such conformational polymorphisms have been proposed to reflect the conformational heterogeneity of the monomer.

Using Atomic Force Microscope (AFM) force spectroscopy, we investigated the conformational equilibria of mouse (Mo) prion protein (PrP) using two different polymeric protein constructs.

Materials and Methods

Heteropolymeric protein constructs flanked by GB1 domains bearing one MoPrP molecule from residue 89 to 230 $(GB1)_4$-$(MoPrP_{89\text{-}230})$-$(GB1)_4$ and four MoPrP molecule copies *in tandem* $(GB1)_2$-$(MoPrP_{89\text{-}230})_4$-$(GB1)_2$ were cloned inside pET11a between BamHI and NdeI restriction sites. Proteins were expressed in BL21(DE3) *E. coli* cells, first purified by SEC and then by Ni^{2+} affinity chromatography. Proteins were concentrated to 1-10 µM and stored in Tris 20 mM pH7.4 NaN_3 0.05% at +4°C.

Constant velocity mechanical unfolding experiments were performed with a Veeco Picoforce AFM on a Multimode Nanoscope IIIa (Bruker) using gold-coated triangular silicon nitride cantilevers (NPG, Bruker) with nominal spring constants of 0.06 N/m. The effective spring constant was determined by characterizing the thermal noise spectrum. Ten microliters of protein specimen was deposited on a flame-cleaned glass coverslip, mounted on a fluid cell and equilibrated with buffer. Pulling velocity was 2180 nm/s. Refolding experiments were carried out by stretching the protein to a fixed length, refolding it at low force for 50 ms and eventually stretching it again; the second unfolding pulse was evaluated.

Analysis was performed by custom designed software [1]; curves were selected depending on the number of GB1 unfolding events and molecule length. Force peaks were fitted using the worm like chain (WLC) model.

Results and Conclusions

In order to establish the conformational heterogeneity of the monomeric MoPrP, we performed pulling experiments using the construct bearing one $MoPrP_{89\text{-}230}$ molecule flanked by four GB1 domains, denoted TR_{x1}. We analyzed the behavior of the construct under different buffer conditions, particularly at different pH and ionic strength, since these two factors are known to modulate the transition from the α-helical form to the β-enriched one [2,3]. Among all recorded single-molecule unfolding events, less than 21 % showed signals not interpretable as GB1 unfolding event (as they show event lengths >30 nm) (Table 1). This finding suggests that a fraction of the sampled PrP molecules might be in a β-enriched and stable structure, rather than in the native α-helical form. Experiments of mechanical unfolding following refolding showed a reduced proportion of such events, probably due to the longer folding time required by β structures.

To understand how more monomeric PrP molecules associate with each other, we pulled the construct bearing four tandem copies of MoPrP molecules in a head-to-tail orientation, denoted TR_{x4}. Interestingly, more than 70 % of the molecules exhibited a strong mechanical behavior (Table 1), which had different lengths and forces (Figure 1). Many of these unfolding events were longer than the unfolded monomeric protein, hence suggesting that strong associations among PrP molecules inside the same polypeptide chain occur. Refolding of such constructs confirmed the presence of strong associations among protein monomers, some of which encompassed the whole length of the four-tandem repeats of MoPrP, indicating that long-range contacts can be established as well. Finally the presence of mild ionic strength (150 mM NaCl) inhibited the formation of such structures only during refolding, suggesting that salt bridges play a major role in the early stages of the association process.

All the data we collected indicate that PrP can undergo conformational changes in the monomeric form, but this is a rare event. The presence of more PrP molecules along the same polypeptide chain can induce them to associate and the buffer can modulate these interactions.

Protein	Experiment	Buffer			
		Tris 20 mM pH 7.4	NaOAc 20 mM pH 5.5	NaOAc 20 mM pH 4.0	PBS pH 7.4
TR_{x1}	Unfolding	20.3 %	13.1 %	16.9 %	-
	Refolding-	17.9 %	13.3 %	4.5 %	-
TR_{x4}	Unfolding	71.6 %	78.9 %	66.7 %	70.3 %
	Refolding-	71.4 %	100 %	-	43.2 %

Table 1. Percentage of unfolding events from prion protein on the overall curves

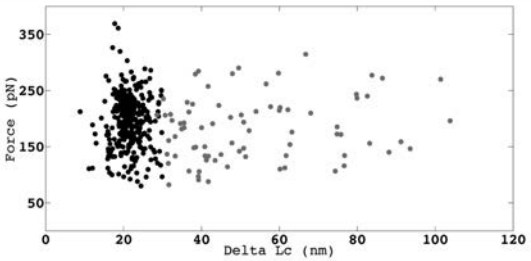

Figure 1. Scatterplot from TRx4 unfolding experiments: GB1 distribution (black dots) and PrP events (gray dots).

References

1. D. Aioanei, et al. Bioinformatics. 2011;27:423
2. L. Calzolai. J Biol Chem. 2003;278:35592
3. A.C. Apetri. J Biol Chem. 2003;278:22187

Substrate topography and heterogeneous nucleations in ion induced dewetting

L. Repetto, R. Lo Savio, E. Piano, G. Firpo, U. Valbusa

Physics Department and Nanomed Labs, Università di Genova, Via Dodecaneso 33, 16146 Genova, Italy

Corresponding author: L. Repetto
E-mail: luca.repetto@unige.it

Keywords: ions, dewetting, nucleations.

Introduction

Thin metal films under ion irradiation undergo morphological modifications that cannot be simply ascribed to atom sputtering. In particular, experimental evidence indicates that for a proper combination of film and substrate materials and ion species and energy, the morphology evolution during bombardment can be considered a dewetting phenomenon [1,2]. In fact, as it happens for liquids [3], and metal films that have been brought to a molten state by laser irradiation [4], the film can dewet from his substrate following two different mechanisms: heterogeneous nucleation and spinodal dewetting. In this paper, we will focus on the former mechanism and we will show how the substrate topography can make it favorable with respect to spinodal dewetting. In particular Atomic Force Microscopy (AFM) has been used to acquire the topography of the substrates used in the dewetting experiments, and these data will be employed in numerical simulations implementing a model where the dewetting is induced by the concurrent and contrasting actions of surface tension and Van der Waals forces on the local molten patches produced by the ion impacts [1]. The resulting simulated dewetted patterns show heterogeneous nucleations as it happens in the experiments whereas simulations employing numerically generated substrates, with the same RMS roughness, but without the characteristic features of real substrates, can only produce patterns of spinodal dewetting.

Materials and Methods

Silicon substrates were prepared according to the procedure described in [1] and their surface topography was analyzed by AFM, by using a Dimension 3100 microscope (Veeco Instruments, Plainview, USA) equipped with the Hybrid XYZ closed-loop scanner, and operating in tapping mode. Figure 1 (a) and (d) show two typical topographies whose roughness analysis gives RMS values of 0.19 nm and 0.26 nm respectively.

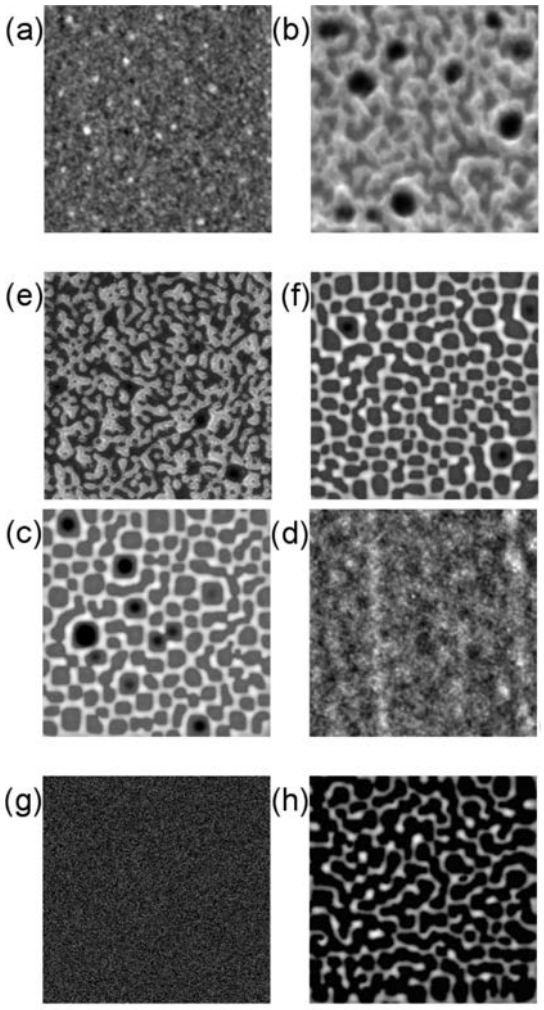

Figure 1. (a) and (d) AFM topographies of two different silicon substrates. (b) and (e) SEM images of 30 keV Ga ion induced patterns for 10 nm Cr films deposited on the substrates in (a) and (d). (c) and (f) corresponding simulations, using the experimental substrate in (a) and (d), where a dewetting phenomenon is induced by the concurring actions of surface tension and Van der Waals forces. (g) numerical white noise substrate and corresponding simulated dewetting pattern. Each panel has a width of 1.5 μm. AFM images z-scale ranges from 0 to 2 nm.

The topography in (d) is rather uniform, while isolated, elevated regions, with a typical height of

0.8 nm, are present on the surface of the former substrate, probably caused by residues of the cleaning procedure. No further action was taken for their removal, as they could serve as possible nucleation centers for the subsequent dewetting experiments. On these substrates we deposited a 13 nm chromium film by a turbo pumped magnetron sputtering system (Emitech K575X, Emitech Ltd., Ashford, Kent, UK) equipped with a quartz crystal microbalance for stopping the deposition at the desired thickness. The samples so obtained underwent ion irradiation with 30 keV Ga ions in a focused ion beam-scanning electron microscopy (FIB-SEM) system (CrossBeam 1540xb, Carl Zeiss AG, Oberkochen, Germany). The ion beam was impinging at normal incidence in a rastering beam with a spot defocused to an 800 nm diameter (size much wider than the chosen pixel size of 12 nm). SEM imaging was performed during the irradiation in order to follow the film morphology evolution in real time.

Results and Conclusions

In Figure 1 (b) and (e) we report the SEM images of the patterns produced by the ion irradiation of the Cr films deposited on the substrates whose topography is shown, respectively, in panels (a) and (d). It is evident as different substrates can favor the occurrence of heterogeneous nucleation as in (b) rather than an evolution of the film morphology according to a spinodal dewetting scheme as in (e). This behavior is confirmed by the simulated patterns, reported in panels (c) and (f) obtained with the program implementing the model described in [1], in this case using the experimental topographies as basis for the simulations. Interestingly, with white noise substrates with comparable RMS roughness (Figure 1 (g) and (h)), heterogeneous nucleations were much more difficult to be identified in simulations (as dry patches occurring in advance with respect the spinodal dewetting). We believe that this behavior is caused by the different spectral weights in the substrate topography, which in the experimental case can show a local unbalance towards longer wavelengths.

In conclusion, we showed that the substrate topography has a prominent role in determing if a thin metal film can undergo spinodal dewetting rather than dewetting by heterogeneous nucleations under ion irradiation. This result can be used to determine the proper experimental conditions for the fabrication of functional surfaces by ion irradiation of thin solid films.

References

1. L. Repetto, et al. Appl Phys Lett. 2012;100:223113
2. L. Repetto, et al. Nucl Instrum Meth B. 2013;315:244
3. R. Xie, et al. Phys Rev Lett. 1998;81:1251

Morphological investigation of Ziegler-Natta catalyst supports

R. Selleri, M. Casinelli

Basell Polyolefine Italia SrL, a LyondellBasell Company, G.Natta Research Center, 44122 Ferrara, Italy

Corresponding author: R. Selleri
E-mail: roberta.selleri@lyondellbasell.com

Key words: catalyst supports, morphology, atomic force microscopy.

Introduction

The ZieglerNatta catalysts, discovered in 1954 by Karl Ziegler and Giulio Natta - awared the Nobel Prize in Chemistry 1963 for their discoveries in the field of the chemistry and technology of high polymers - are the basis for the industrial production of polyolefins.

Starting from the earlier titanium trichloride based catalysts, the discovery of magnesium chloride as the election support for titanium tetrachloride and of the routes to obtain a control of particle morphology represented the most important breakthrough for the development of modern catalysts. Now, the complete control of morphology from the support to the catalyst and, finally to the growing polymer particles represent a key point in leading industrial polymerization processes. [1]

In this study a morphological investigation based on an interdisciplinary approach involving different microscopy techniques was used, made possible by the setup of a new sample preparation procedure. The combination of the complementary information brought about a deepen awareness of the observed morphology.

Materials and Methods

Catalyst supports

The materials used for this study are supports produced in our industrial plants that differ for the residual final composition in term of Ethanol content, in association with the catalyst derived from one of the selected supports. All materials were investigated as for surface and section morphology knowledge. The sample preparation procedure requires all steps performed under inert atmosphere, with an improved analytical method for the section investigation, based on sample embedding in proper low viscosity resin plus cutting with Ultracryomicrotome apparatus.

Equipment

Scanning Electron Microscope

Samples were examined on ESEM Quanta 200 FEG (FEI) using the low vacuum mode and the solid state detector, imaging the backscattered electrons originated by the interaction between the sample and the primary beam. EDS analysis was also performed by Bruker XFlash® 5030 (SDD detector) as in semi quantitative mode and in map one.

Atomic Force Microscopy

The same specimen samples investigated by ESEM have been further analyzed by Nanoscope V (Bruker) under inert atmosphere, collecting amplitude and phase data by using Bruker silicon tapping probe RTESP model.

Transmission Electron Microscopy

A Tecnai 10 (FEI) apparatus was used to image the sample after a manual milling in a crucible and suspension in anhydrous hexane.

Results and Conclusions

The ESEM analyses performed on the selected samples prepared under inert atmosphere have confirmed the presence of a network type inner morphology with presence of porosity channels. By the use of EDS maps the channels have been uniquely identified allowing further Image Analyses interpolation for quantitative measurements of their mean diameters.

The same sample sections identified by ESEM were investigated by AFM in tapping mode at high magnification. Interesting differences between support and catalyst intrinsic morphology have been revealed, showing a granular structure with differences in dimension and shape as reported in Figures 1 and 2.

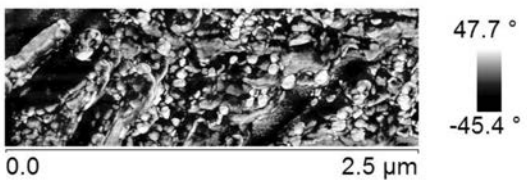

Figure 1. AFM phase image of support.

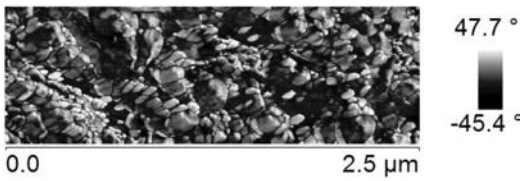

Figure 2. AFM phase image of derived catalyst.

The granular structure morphology has been confirmed also by TEM analyses

The present study has showed that an interdisciplinary approach with different microscopy techniques applied on the same prepared specimen is able to catch the catalyst supports primitive morphology directly on real spherical samples from plant productions. The obtained results of porosity network by ESEM and granular structure by AFM and TEM are in line with data literature on lab scale samples [2].

In particular the AFM technique thanks to its atomic resolution has evidenced the intrinsic granular structure of catalyst supports allowing further studies of correlation between plant process conditions and obtained morphologies.

References

1. G. Cecchin, et al. Macromol Chem Phys. 2001;202:1987.
2. A. Andoni, et al. J Catalysis. 2007;247:129.

A new method for simultaneous Shear Force and Radiofrequency-Microwave analysis in Scanning Probe Microscopy: morphological, viscoelastic and dielectric properties of materials

G. Valdrè, D. Moro

Department of Biological, Geological and Environmental Sciences, Alma Mater Studiorum - University of Bologna, P. di Porta San Donato 1, Bologna 40126, Italy

Corresponding author: G. Valdrè
E-mail: giovanni.valdre@unibo.it

Key words: radiofrequency, microwaves, shear force microscopy, vertically oriented cantilevers.

Introduction

We present a novel method that allows the simultaneous acquisition of the sample topography and viscoelastic and dielectric ε(ω) properties at the nanoscale. The low force of probe-to-sample interaction, characteristic of the shear force mode of operation, opens to the easy investigation of biological matter and more in general of soft samples minimizing the specimen deformation, damaging and dislodging. The shear force method also provides the viscoelastic properties of the sample surface and of thin liquid films nanoconfined between the probe apex and the underneath sample area. To this purpose we used a microcantilever set with its long axis perpendicular to the specimen surface (VOC, vertically oriented cantilever configuration). The morphology of the specimen is thus acquired using the shear force signal variation between the sample surface and the VOC apex that is excited to oscillate in a direction parallel to the sample surface. The probe is only sensitive to horizontal forces (shear forces) because of the high vertical spring constant of the cantilever.

Then, in order to acquire dielectric ε(ω) and RF-microwave material-related properties we have connected the VOC to a vector network analyzer, VNA (RF range 100 kHz–8.5 GHz) to measure RF impedance signal variations at the VOC apex-sample interface or through the specimen thickness [1, 2]. The VOC probe-to-sample configuration is very important because minimizes the parasitic capacitance of the cantilever.

Materials and Methods

A Multimode® atomic force microscope, AFM (Digital Instruments Inc., Santa Barbara, CA, USA), interfaced with a Nanonis AFM control system (Nanonis: SPECS Zurich GmbH, Zurich, Switzerland) equipped with two oscillation controller modules (with digitally integrated PLL/lock-in), was modified to perform shear force microscopy [1]. The vertically oriented cantilever, VOC, was connected to an Agilent ENA 5071C vector network analyzer (Agilent Technologies Inc., Santa Clara, CA, USA). To perform RF analysis, the microwave signal generated by the VNA is transmitted to the VOC and part of the signal is reflected (or transmitted) depending on the probe-to-sample impedance mismatch (or through specimen properties). The probe-to-sample mismatch variation is dependent on the material local properties of the sample and on the probe-to-sample distance at the nanoscale. For instance, the ratio of the generated microwave signal and the reflected one is measured by the VNA as a scattering reflection signal, S_{11}. The complex scattering parameter S_{11} is related to the probe-to-sample impedance by the following equation:

$$S_{11} = \frac{Z_L - Z_0}{Z_L + Z_0}$$

where Z_0 is the characteristic impedance of the transmission line, typically 50 Ω , and Z_L is the load impedance, which is equivalent to the impedance at the probe-to-sample interface. Through the VNA, we measured the variation of the modulus $|Z_L|$ and phase θ of the complex impedance $Z_L = |Z_L|e^{i\theta}$ at the probe-to-sample interface.

Results and Conclusions

1) Polystyrene spheres, muscovite crystallographic steps and DNA single molecules were used to test the performance of the shear force mode. The polystyrene spheres, with a mean diameter of 194 nm ± 5%, were used for the x–y calibration, whereas the stacking of 1 nm thick layers of the crystal structure of a commercial muscovite was used to test the z resolution of the system. The spatial resolution of the shear force mode in biomolecular imaging was assessed using as a test specimen DNA single molecules deposited on an atomic flat substrate. These observations

demonstrated the reliability of the shear force device and the low induced deformation, damaging and dislodging when dealing with biological matter and more in general with soft materials [1].

2) We used atomic flat graphite with the nanosized polystyrene spheres onto to test the simultaneous shear force and RF-microwave method. Impedance spectra were acquired in the frequency range from 100 kHz to 8.5 GHz [2,3].

We found a strong dependence of the RF impedance phase θ from both the probe-to-sample distance and the type of material (graphite or polystyrene). The RF impedance signal was highly sensitive to very short probe-to-sample distances (Figure 1), with an exponential trend that follows the empirical formula:

$$\theta(z) = a \cdot e^{-b \cdot z} + c$$

where z is the probe-to-sample distance, a, b and c are calibration parameters.

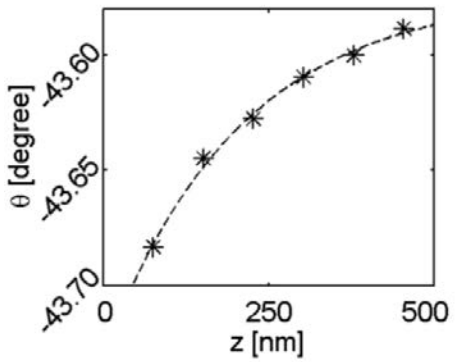

Figure 1. Exponential approximation (dashed line) of the experimental trend (stars) of the RF impedance phase signal versus the probe-to-sample separation z.

Through shear force and RF impedance variation analysis we performed a detailed characterization of the probe-to-sample shear nanocontact, where the sensing element for both the shear force and the radiofrequency signals is the apex at the free end of the VOC. The probe was characterized to behave like a capacitive non-contact probe during shear force observations, at least for frequency <100 MHz. Whereas, the impedance shows a highly variable signal characteristic of the type of cantilever and the experimental set-up at high frequency (>100 MHz).

In our configuration at a fixed RF, dynamic experiments of approach and withdrawal of the probe revealed a switch-like behavior related to a drastic change of the impedance from a non-contact/engage-contact regime to the contact regime which nullifies the free mechanical oscillation amplitude of the cantilever. Different types of cantilevers presented similar trends of the impedance modulus and phase as a function of the probe-to-sample distance, being the Δθ variation independent of the cantilever length and shape.

It is expected that the versatility of the presented Shear Force and RF-Microwave SPM-based method will be of great help to investigate the nanoscale morphology, viscoelastic and dielectric ε(ω) properties of a wide spectrum of materials, from metallic to dielectric and biological matter. Further work is ongoing to develop a quantitative methodology using calibrated standards.

References

1. G. Valdrè, et al. Meas Sci Technol. 2012;23:085903
2. G. Valdrè, D. Moro. Rev Sci Instrum. 2012;83:126103
3. G. Valdrè, D. Moro. Meas Sci Technol. 2013;24:095901

Scanning electron microscopy in monitoring the aging of alternative materials for plastering of canvas manufactured products

S. Burattini,[1] L. Baratin,[2] L. Borgioli,[4] L. Sabatini,[3] S. Orsini,[5], V. Viti,[2] E. Falcieri,[1] D. De Luca[2]

[1]DiSTeVA, [2]Scuola di Conservazione e Restauro, DiSBEF and [3]DiSB; Università degli Studi di Urbino Carlo Bo, Italy; [4]Opificio delle Pietre Dure di Firenze and CTS srl, Altavilla Vicentina, Italy; [5]DiCCI Università di Pisa, Italy

Corresponding author: Sabrina Burattini
Dipartimento di Scienze della Terra, della Vita e dell'Ambiente (DiSTeVA) Università degli Studi di Urbino Carlo Bo, Campus Scientifico "Enrico Mattei" via Ca' Le Suore, 2; 61029 Urbino, Italy
Tel. +39.0722.304311 - Fax: +39.0722/304244
E-mail: sabrina.burattini@uniurb.it

Summary
During the restoration of manufactured canvas, the plastering of recoverable lacunae is generally carried out by means of dehydrated *gesso*, rabbit-skin glue or, more rarely, by using already made up products. Being gesso-animal glue mixture totally comparable with canvas constitutive materials, it must be considered the strong drying correlated shrinkage, the poor mechanical resistance and the possibility to be a substrate for deteriorating biological agents, in particular environmental conditions. Similarly, ready-to-use products, such as Modostuc and Polyfilla, undergo a dramatic shrinkage and show a poor mechanical resistance. Aquazol®, BEVA® *gesso* and Balsite®, new products commonly used for different purposes, have been here analyzed. Their behavior has been studied by careful light microscopy observation of their chromatic changes and by scanning electron microscopy of their surface details. An artificial aging condition was also induced to better characterize their response to the environmental damage progression. The performed studies on these materials provided very positive results and their potential use in the place of common use fillers has been suggested.

Key words: heritage, restoration, aging, canvas, lacunae filling.

Introduction

Materials used for lacunae filling in textile paintings must be closely comparable with constituents, in terms of chemical composition, plasticity, hardening speed, elasticity, painting appropriate surface and progressive shrinkage. Moreover, they must show a relative resistance to possible mechanical damage, microbial contamination, aging or sun radiations.

Currently few materials, considered appropriate for lacunae filling, are available and animal glue, Modustic and Polyfilla are now commonly utilized. The use of a filling plaster, composed by a proteinaceous binder and an inert (rabbit-skin glue-*gesso*), has been now also consolidated in the common practice. Its characteristics are indeed closely comparable to manufactured product ones. Nevertheless, in the last years it has been demonstrated to be less flexible and more susceptible of microorganism contaminations (Fuster-Lopez *et al.* 2006; Appolonia *et al.* 2009, 2010; Coppola *et al.* 2011).

In this study some relatively new products have been studied by scanning electron microscopy (SEM) in basic control condition and after the experimental laboratory induction of an artificial accelerated aging.

Materials and Methods

Materials

In this study, we have analyzed Aquazol®, BEVA® *gesso* and Balsite®, products generally used for different purposes (adhesive or fillers), even if in the same field of art manufactured prod-

ucts. In previous studies such substances had been set up on textile supports to submit them to specific tests of workability of the fillers, dimensional shrinkage, suitability to the reintegration painting and varnishing, mechanical strength, reversibility and finally resistance to the most common biodeteriogens agents (Calore *et al.* 2011; Viti *et al.* 2011; De Luca *et al.* 2012, 2013).

Sample aging conditions

Critical conditions of temperature and humidity have been experimentally applied to the materials. For that A Solar Box 1500e RH, (Erichsen, Italy), purchased from Erichsen (Germany), was used for the artificial aging (A). The aging conditions were as follows: 50°C, excitation with a Xenon lamp (wavelength 280-400 nm), radiation power 650W. The behavior of the materials has been studied after three weeks of warm/moist conditioning cycles (90% RH for 72h), alternated with 144 h at 50% atmospheric humidity. A Soda-lime glass UV filter was used to simulate indoor exposure.

SEM analysis

The dimensional shrinkage of tested products has been evaluated by means of SEM (Philips 515), with the aim to study surface changes after aging chamber.

To exclude alterations due to technical procedures, no *critical point drying*, nor *gold-sputtering* have been carried out (Burattini *et al.*, 2013). Therefore, original uncoated samples have been directly mounted on graphite/adhesive tap-coated stubs. All pictures (1cm x 1cm) have been performed at the same magnification, at the same high tension (15 kV) and by taking care in maintaining the same sample tilting before and after aging procedure, even if different in the four samples. Particular reference structures were chosen to ensure the correct comparison of the two experimental conditions.

SEM analysis of microbiological contamination has been performed after air drying and gold-sputtering (Salucci *et al.*, 2013).

Monitoring of microbiological contamination

The observations of samples has been carried out by means of a Zeiss Axiolab Hbo 50/AC, with a 40x objective, at a final 400x magnification, as well as by SEM.

Results

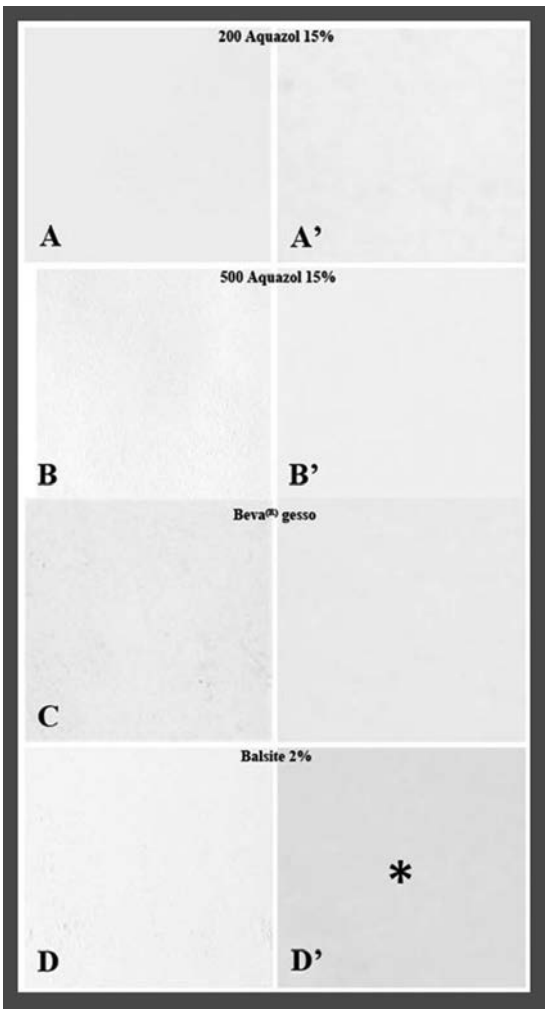

Figure 1. Chromatic changes before (A,B,C,D) and after (A',B',C',D') artificial accelerated aging of 15% Aquazol® 200 (A,A'), 15% Aquazol® 500 (B,B'), BEVA® *gesso* (C,C') and 2% Balsite® (D,D'): only in Balsite® specimens a chromatic changes can be revealed (*).

Compared to results obtained in the previous experiments, the products do not show a further dimensional shrinkage due to artificial aging and most of them, except for Balsite®, have no significant color changes (Figure 1). When plasters were obtained with 15% Aquazol® 200 or 15% Aquazol® 500, the samples appear fragile and strongly affected by sun irradiation or thermo-hygrometric damage. A number of surface deformations or signs of material breaks appear indeed (Figures 2 and 3). No chromatic changes before and after artificial ageing appear (Figure 1A, A' and 1B, B'). With regard to BEVA® *gesso*, both consistence and aspect appear good: in fact, the ready-for-use product made with EVA resins does not reveal aging-related deformations, fractures (Figure 4) or significant chromatic changes (Figure 1D, D'). The best results are observable in samples plastered with 2% ethanol Balsite® mixed with 15% white titanium pigment. SEM observations show that signs of mechanical changes are absent. Moreover, if compared to initial conditions of the pure product, no dimensional reduction or changes due to pigment addition, appear (Figure 5). However, the plaster shows a moderate chromatic alteration after the experimental induction of aging, revealing an amber-like tone (Figure 1C,C').

Despite its aging resistance, an unexpected behavior was observed with Balsite® fillers, which showed an important fungal growth (≥ 60),

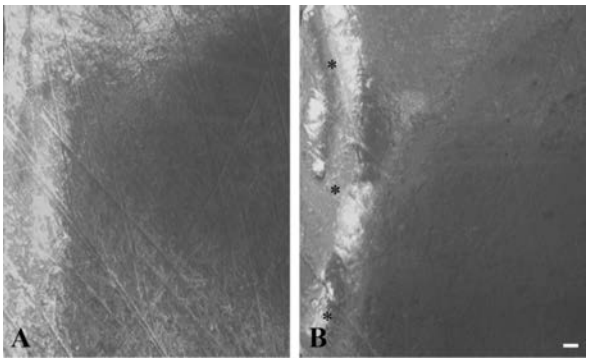

Figure 2. SEM of samples plastered with 15% Aquazol® 200, before (A) and after (B) artificial aging: localized surface swellings (***) appear after the treatment. A,B, Bar=0.4 µm.

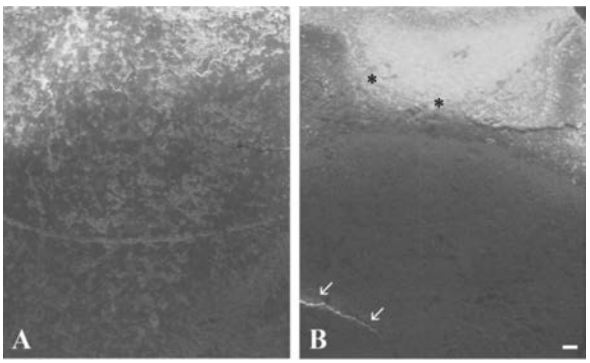

Figure 3. SEM of samples plastered with 15% Aquazol® 500, before (A) and after (B) artificial aging: a localized surface swelling (**) and occasionaly breaks (→) appear after the treatment. A,B, Bar=0.4 µm.

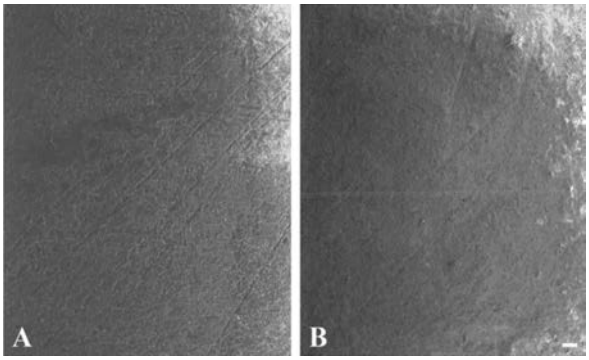

Figure 4. SEM of samples plastered with BEVA® gesso before (A) and after (B) artificial aging: no effect is evident. A,B, Bar=0.4 µm.

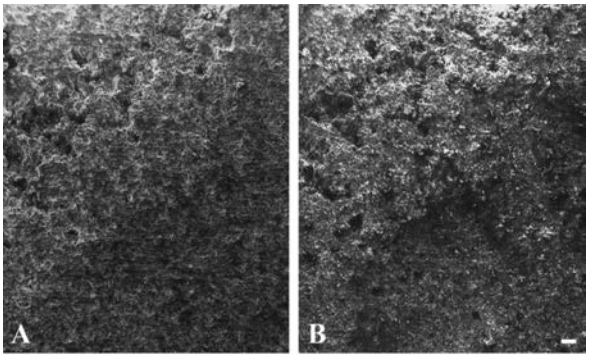

Figure 5. SEM of samples plastered with 2% ethanol Balsite® and stained with 15% pigment, before (A) and after (B) artificial aging: no effect appears. A,B, Bar=0.4 µm.

in which microscopic analysis identified *Aspergillus niger* and *Aspergillus spp* (Figure 6).

SEM observations confirmed the presence of a fungal contamination (Figure 7).

A possible cause of this problem are phloem fibers, hemp or flax, added to the products in order to increase their lightness, and potentially creating a more favorable environment to fungal growth. To this regard, the manufacturer of Balsite® has changed the plaster formulation by inserting a suitable biocide, the efficacy of which was reported by De Luca *et al.*, 2013.

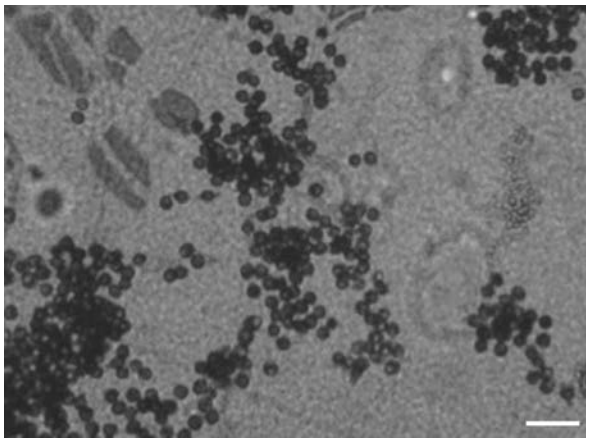

Figure 6. *Aspergillus* niger and *Aspergillus spp* appear on Balsite® plastered samples. Bar=25 µm.

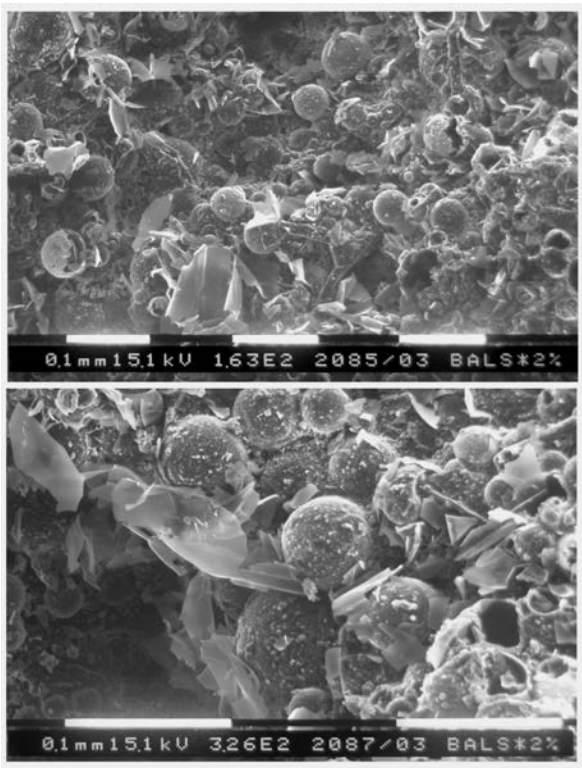

Figure 7. Balsite® plastered samples SEM of *Aspergillus niger* and *Aspergillus spp.*

Discussion

These observations demonstrate that Aquazol®, BEVA® *gesso* and Balsite® evidentiate the most significant results. However, for 200 and 500 Aquazol® products, a screen obtained by means of a special layer (back and front side consolidant application) is necessary, as generally used when the materials are utilized as consolidants. Moreover, a careful evaluation of preservation conditions, both from thermo-hygrometric or sun damage, is strongly recommended. If compared to ready-to-use Modostuc and Polyfilla commercial products, but also to common plasters

obtained with *gesso* and animal glue, here described products show high quality mechanical, chemical and physical characteristics. Therefore, they can be considered excellent and ecologically compatible substitutes of animal glue.

Acknowledgements

The research was supported by Urbino University. We thank Francesca Modugno and Giulia Papini for their help and critical suggestions. The technical assistance of Oliviero Rusciadelli and Lorenzo Bedini is also greatly appreciated.

References

Appolonia L, Pinna D, Cauzzi D, Casoli A, Campani E, Berzioli M, et al. Studio per la caratterizzazione chimico-fisica dei consolidanti. Valutazione della variazione delle proprietà chimico-fisiche con l'invecchiamento artificiale di undici adesivi, di origine naturale e sintetica, comunemente utilizzati come consolidanti nel restauro di beni storico-artistici. Atti del convegno "L'attenzione alle superfici pittoriche. Materiali e Metodi per il Consolidamento e Metodi Scientifici per Valutarne l'Efficacia", CESMAR7 (a cura di) Milano, 21-22 nov. 2008, Il Prato, Padova 2009; 9-32.

Burattini S, Falcieri E. Analysis of cell death by electron microscopy. Methods Mol Biol. 2013;1004:77-89.

Calore R, Frizza L, Jaxa-Chamiec M, Rizzonelli L, Stevanato N, Tisato F. Aquazol® 500. Una possibile alternativa ecocompatibile alla colla animale nella preparazione degli stucchi per il restauro dei dipinti. Test preliminari per la stabilità, lavorabilità e comportamenti, in "Colore e conservazione. Le fasi finali nel restauro delle opere policrome mobili", Atti del congresso, Trento 19-20 novembre 2010, Il Prato, Padova 2011; 79-86.

Coppola A, Digennaro G, Lavenuta G. Confronto tra i comportamenti di materiali tradizionali e di materiali innovativi utilizzati nelle fasi finali degli interventi di restauro dei dipinti su tela, in "Colore e conservazione. Le fasi finali nel restauro delle opere policrome mobili", Atti del congresso, Trento 19-20 novembre 2010, Il Prato, Padova 2011; 69-78.

De Luca D, Borgioli L, Burattini S, Orsini S. Manufatti dipinti su supporto tessile: proposte di materiali alternativi per la stuccatura delle lacune. Comportamento all'invecchiamento, in «Kermes», 89, Nardini, Gennaio-Marzo 2013 (Submitted)

De Luca D, Borgioli L, Sabatini L, Viti V. Manufatti dipinti su supporto tessile. La reintegrazione delle lacune: proposta di materiali alternativi in «Kermes», 88, Nardini, Ottobre-Dicembre 2012; 42-54

Fuster-Lopez L, Mecklenburg MF. Materiali per la stuccatura nei dipinti mobili: materiali tradizionali e moderni verso una valutazione critica dell'idoneità, stabilità e versatilità delle formulazioni tradizionali ed attuali, in "Colore e conservazione. Le fasi finali nel restauro delle opere policrome mobili", Atti del congresso, Trento 19-20 novembre 2010, Il Prato, Padova 2011; 45-56.

Fuster L, Mecklenburg MF, Castell-Augusti M, Guerola-Blay V. Idoneità meccanica degli stucchi usati nel riempimento di mancanze di dipinti su tela, in "Lo Stato dell'Arte 4. Congresso nazionale IGIIC, Sessione Poster", Nardini, Siena 2006; 599-608

Viti V, Borgioli L, De Luca D, Sabatini L. Restoration of lacunae on textile heritage: proposal of alternate materials, 10th Multinational Congress on Microscopy 4-9 settembre 2011 Urbino, Campus scientifico, Università degli Studi Carlo Bo.

Salucci S, Burattini S, Baldassarri V, Battistelli M, Canonico B, Valmori A, et al. The peculiar apoptotic behavior of skeletal muscle cells. Histol Histopathol 2013;28:1073-87.

Autofluorescence and metabolic signatures in a pig model of differentiation based on induced pluripotent cells and embryonic bodies

A.C. Croce,[1] G. Bottiroli,[1] G. Santin,[1] G. Pacchiana,[2] P. Vezzoni,[2] E. Di Pasquale[2]

[1]IGM-CNR and Department of Biology and Biotechnology, University Pavia, Pavia 27100, Italy
[2]Humanitas Clinical and Research Center and IRGB/CNR, UOS of Milan, Rozzano 20089 (MI), Italy

Corresponding author: Anna Cleta Croce
Istituto di Genetica Molecolare del CNR c/o Dipartimento di Biologia e Biotecnologie "L. Spallanzani", via Ferrata, 9
27100, Pavia, Italy
Tel. +39.0382.986428 - Fax +39.0382.986430
E-mail: croce@igm.cnr.it

Summary
Besides several genetic and molecular markers, stem cells undergoing differentiation show changes in their metabolic engagement, such as a switch from anaerobic to aerobic energetic metabolism and decreased autophagic activity, representing metabolic signatures of the stemness status. These activities involve biomolecules - respectively NAD(P)H and flavins, and lipofuscin-like lipopigments- that give rise to autofluorescence (AF) emission under suitable excitation light conditions. Since these endogenous fluorophores can be exploited as cell intrinsic biomarkers, attention is currently deserved to assess the potential of AF analysis to monitor the cell stemness status or maturation degree into a desired phenotype. In our work, we employed pig induced pluripotent stem (iPS) cell as a model of differentiation to compare their AF properties in living conditions with those of embryoid bodies (EBs) derived from them, by means of imaging, microspectrofluorometric techniques and spectral fitting analysis. The AF results indicate that reprogramming of suine iPS cells do not lead to typical metabolic functions of the undifferentiated status. These findings support the value of AF analysis as a tool for a comprehensive assessment of the actual stem cells differentiation degree in the development of regenerative medicine strategies, and for application to animal species of interest in veterinary, zootechnology and, in general, to the species for which immunomarkers are not yet available.

Key words: aerobic/anaerobic metabolism, lipofuscin-like lipopigments, microspectrofluorometry, stem cells.

Introduction

The natural presence of biomolecules acting as endogenous fluorophores is responsible for the autofluorescence (AF) emission rising from cells and tissues when submitted to a suitable excitation light. The strict involvement of endogenous fluorophores in metabolic reactions influences their amount and physicochemical state, in turn affecting their emission properties. As a consequence, the overall cell AF emission signal carries multiple information, making endogenous fluorophores to act as intrinsic biomarkers of the cell functional engagement in the absence of exogenous labeling agents (Ramanujam, 2000; Bottiroli and Croce, 2004).

Besides several genetic and molecular biomarkers, cells undergoing differentiation or reprogramming processes are characterized by a metabolic plasticity based on activities involving endogenous fluorophores and likely affecting AF emission properties (Folmes *et al.*, 2012; Santin *et al.*, 2013) Figure 1. Mitochondria, in particular, play an essential role in the maintenance of stem cell homeostasis, consistently both with the switch from anaerobic to aerobic respiration during differentiation and with the autophagic processes, providing for the removal of undesired cell components to maintain the pluripotent status, the opposite occurring during the somatic to pluripotent cell reprogramming (Hernebring *et al.*, 2006; Wang *et al.*, 2011; Rehman *et al.*, 2010; Chen *et al.*, 2012). The consequent changes in the cell engagement in energetic metabolism influence the amount, redox state and bound-free condition of the coenzymes NAD(P)H and flavins (Croce *et al.*, 1999; Salmon *et al.*, 1982; Kunz *et al.*, 1986). The AF emission properties of these endogenous fluorophores up

to now mainly investigated in energetic metabolism studies (Aubin, 1979; Balaban and Mandel, 1990), have been more recently considered for the assessment of the stemness status of human and animal stem cells. Novel and sophisticated techniques have been applied, including a two photon non invasive autofluorescence imaging tool and a phasor approach for the monitoring of the metabolic state of different living stem cell models (Uchugonova *et al.*, 2008; Rice *et al.*, 2010; König *et al.*, 2011; Stringari *et al.*, 2011; Stringari *et al.*, 2012a,b; Santin *et al.*, 2013). The autophagic activity for the removal of undesired subcellular structures, in turn, is expected to result in an accumulation of lipofuscin like products, that can be detected though their AF emission in the yellow-reddish region (Wolman, 1980; Terman *et al.*, 2006).

The development of regenerative therapies is greatly relying on the use pluripotent cells (Welling and Geijsen, 2013). The induction of pluripotent stem cells (iPS) through the reprogramming of adult elements (Yamanaka, 2009; Cherry and Daley, 2012; Kahler *et al.*, 2013) is likely to be preferred to the use of Embryonic Stem Cells (ESCs), their self-renewal features being retained as long as the culture conditions prevent differentiation, along with the ability to differentiate into all adult cell types through their aggregation into embryoid bodies (EBs) (Evans *et al.*, 1981; Williams *et al.*, 1988; Desbaillets *et al.*, 2000). The use of iPS cells results in enormous advantages since it overcomes the ethical concerns related to the use of human ESCs and, at the same time, it allows in principle to generate pluripotent cells from a broad spectrum of adult somatic cells.

The successful driving of a cell lineage to the desired phenotype entails the correct assessment and monitoring of the stemness status. In this view, the AF analysis can provide data on the metabolic engagement, useful to integrate the transcription and surface-immunological biomarkers as the expression of regulation factors (Nagano *et al.*, 2008; Enver *et al.*, 2009), or at least to characterize cells from animal species for which immunomarkers are not yet available.

In our work we used pig iPS cells, currently highly considered for applications in biomedical and biotechnological fields, and EBs derived from them, to investigate the potential of real time, in vivo and non invasive AF analysis as a supportive tool for a comprehensive assessment and monitoring of the actual differentiation degree.

Materials and Methods

Cell model

Pig iPS cells have been maintained as previously described (Ezashi T *et al.*, PNAS 2009). In brief, pig iPS cells have been grown onto a feeder of inactivate mouse embryonic fibroblasts (MEF) in a medium based on DMEM/F12 and supplemented with 20% Knockout Serum Replacement, Glutamine, non-essential amino acids and basic FGF (4 ng/mL).

To obtain EBs, iPS cells have been first passaged onto gelatin-coated dishes (0.1%) to deplete the MEF feeder in pluripotency medium, and then passaged using Dispase (1 mg/mL) and plated onto ultra-lo attachment plated in a medium containing fetal bovine serum (FBS).

For both AF imaging and microspectrofluorometric analysis, the cells were seeded onto 0.1% gelatin coated glass coverslips in the absence of feeder, to be put upside down immediately before the AF imaging and microspectrofluorometric analyses.

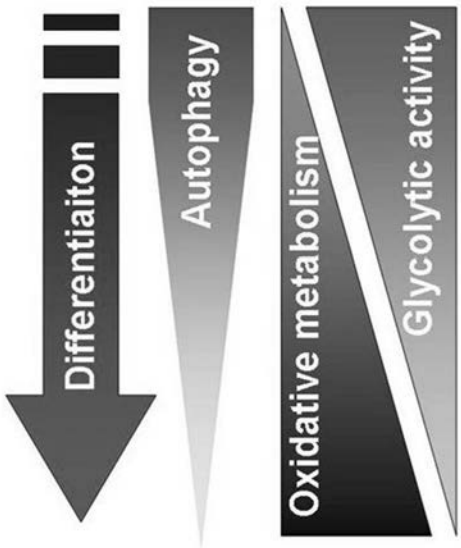

Figure 1. Schematic representation of metabolic signatures and their changes, exploitable for the AF analysis of cell differentiation: aerobic/anaerobic energetic metabolism and endocytosis/autophagy, involving respectively NAD(P)H and flavins, or lipofuscins as endogenous fluorophores.

Autofluorescence image analysis

The AF images were collected by means of an Olympus BX51 fluorescence microscope (Olympus Optical Co. GmBH, Hamburg, Germany), equipped with a 100W Hg excitation lamp and a 4.1 Mpixel digital photocamera (Olympus Camedia C-4040 zoom), the acquisition conditions being: WU Olympus fluorescence cube (330–385 nm band-pass excitation filter, Full Width at Half Intensity Maximum (FWHM) 58 nm), BA420 long-pass barrier filter; oil immersion 100X UplanFl Olympus objective (NA 1.25). Following each AF image collection, bright field pictures were also recorded from the same cells.

Microspectrofluorometric analysis

The AF spectra were recorded under epi-illumination by means of a microspectrograph (Leitz, Wetzlar, Germany) equipped with an Optical Multichannel Analyzer (EG&G - PAR, Princeton, NJ), and a 512-element intensified diode array detector, mod. 1420/512. Excitation light was provided by a 100 W Hg lamp (Osram, Berlin, Germany), combined with KG1-BG38 anti-thermal filters. Acquisition conditions were: 366 nm band-pass interference excitation filter (FWHM 10 nm, $T\%_{366} = 25$), 390 nm dichroic mirror ($T\%_{366} < 2$); 390 nm long pass filter; oil immersion 95X Leitz objective with incorporated iris diaphragm (NA 1.10-1.32).

Spectra were recorded in the 400-680 nm range, 10 sequential scans of 200 ms each for a total of 2 s of acquisition time. To avoid photobleaching effects before measurement, cells were selected and focused at microscope under low bright field illumination.

An iterative non-linear curve-fitting procedure (PeakFit; SPSS Science, Chicago, IL, USA) based on the Marquardt-Levenberg algorithm (1963) was used for the analysis of AF spectra. The procedure is based on a combination of half-Gaussian Modified Gaussian (GMG) spectral functions describing the emission profile of each single fluorophore to evaluate their relative contribution to the overall emission, by means of subsequent adjustments to match the best fit for the experimental spectrum profile, as already described in detail (Croce *et al.*,1999; Croce *et al.*, 2004). The spectral parameters of the single fluorophores considered were: free NAD(P)H (peak center wavelength, λ = 463 nm; FWHM = 115 nm), bound NAD(P)H (λ = 444 nm; FWHM = 105 nm), flavins (λ = 526 nm; FWHM = 81 nm), porphyrins (λ = 635 nm; FWHM = 20 nm), proteins (emission tail, λ<440 nm) and lipofuscin-like lipopigments ($\lambda \approx 587$ nm; FWHM ≈ 80 nm). In the two latter cases, modifications of the spectral functions were allowed, due to the variability of the lipofuscin-like lipopigments emission profile in dependence of their heterogeneous chemical composition *i.e.*, proteins, lipids, carotenoids- oxidation and crosslink degree (Wolman, 1980). The goodness of fitting verified in terms of r^2 coefficient determination, and residual analysis. The relative contribution (%) of each fluorophore estimated from the spectra normalized to 100 (area value, a.u.) was then referred to the real values of the whole emission area. A minimum of 25 cells was measured for each cell type for each sample (minimum, 2 slides).

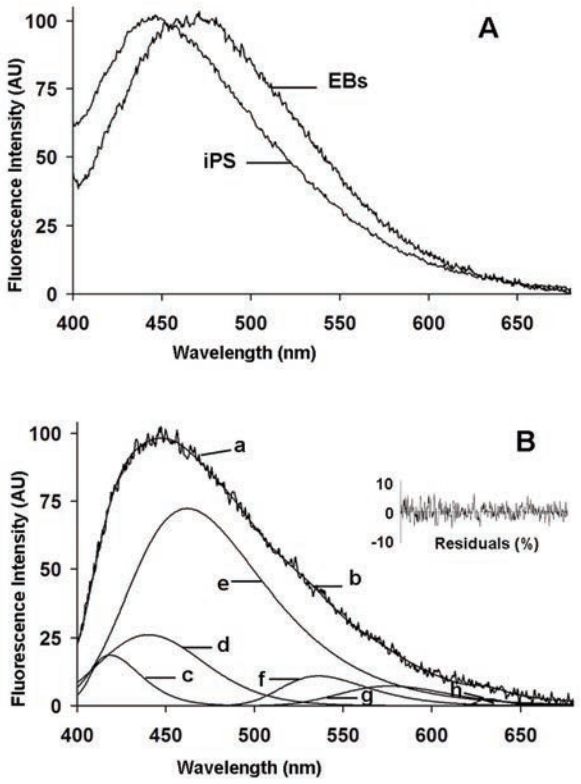

Figure 2. (A) Examples of AF spectra collected from iPS cells and EBs. (B) Example of fitting analysis of an AF spectrum collected from iPS cells. Measured spectrum (a) and calculated curve (b), as the sum of the contribution of the single endogenous fluorophores: proteins (c), NAD(P)H bound (d), NAD(P)H free (e), flavins (f), lipofuscin-like lipopigments (g), porphyrins (h). Insert: residual analysis. Fitting r^2 coefficient of determination ≥0.989.

Results

Microspectrofluorometric analysis

The AF spectra recorded from iPS and EB cells show differences in their emission profile (Figure 2A), that can be ascribed to changes in the relative contribution of the main endogenous fluorophores to the whole AF emission signal (Figure 2B). These changes have been analyzed by means of spectral fitting procedure and the results are presented as bar charts (Figure 3 A-C). In general, the greater contribution to the whole cell emission is given by the coenzyme NAD(P)H, accounting for more than 60%, oxidized flavins accounting for less than 4%, and lipofuscin-like lipopigments for a

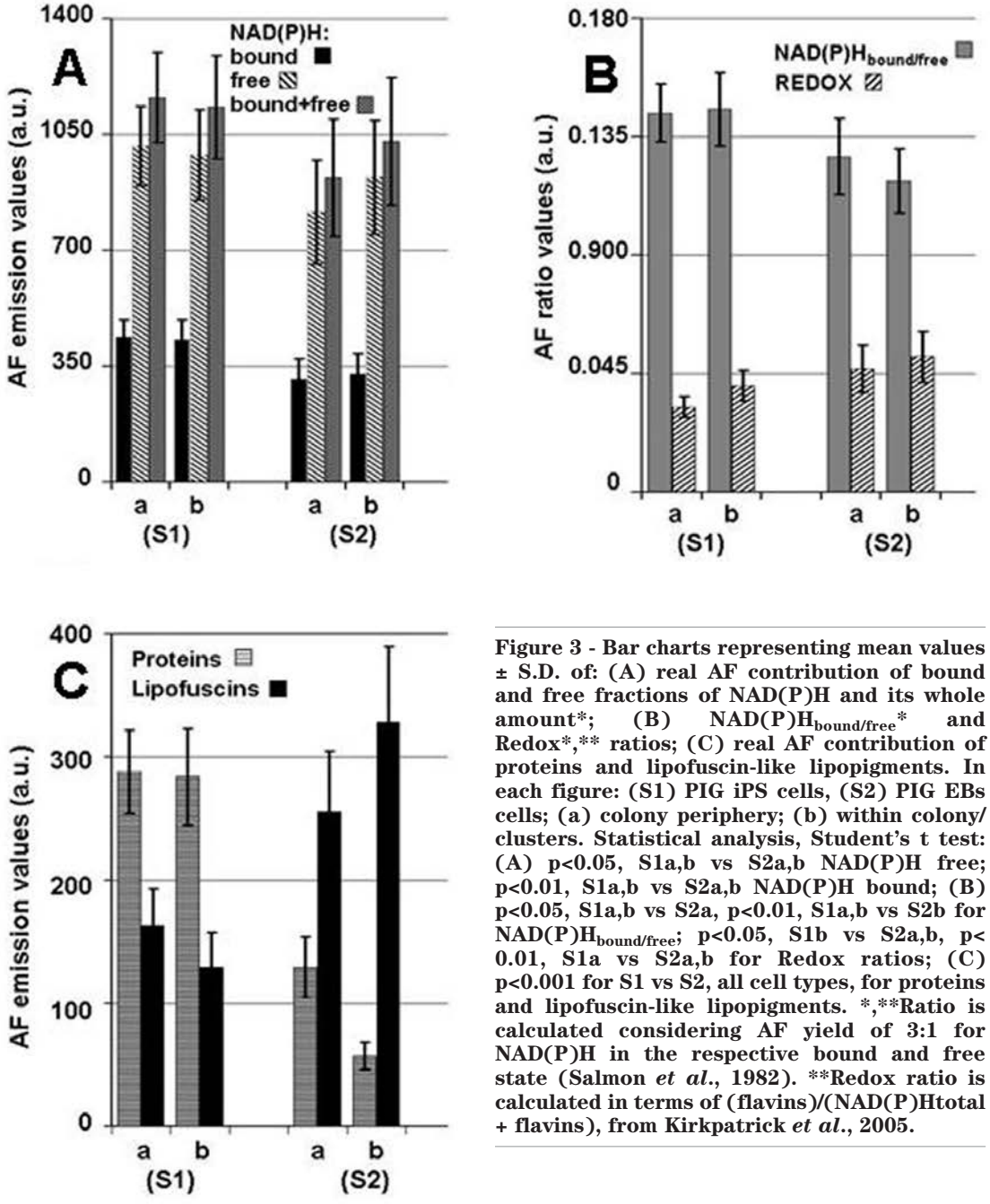

Figure 3 - Bar charts representing mean values ± S.D. of: (A) real AF contribution of bound and free fractions of NAD(P)H and its whole amount*; (B) $NAD(P)H_{bound/free}$* and Redox*, ratios; (C) real AF contribution of proteins and lipofuscin-like lipopigments. In each figure: (S1) PIG iPS cells, (S2) PIG EBs cells; (a) colony periphery; (b) within colony/clusters. Statistical analysis, Student's t test: (A) p<0.05, S1a,b vs S2a,b NAD(P)H free; p<0.01, S1a,b vs S2a,b NAD(P)H bound; (B) p<0.05, S1a,b vs S2a, p<0.01, S1a,b vs S2b for $NAD(P)H_{bound/free}$; p<0.05, S1b vs S2a,b, p< 0.01, S1a vs S2a,b for Redox ratios; (C) p<0.001 for S1 vs S2, all cell types, for proteins and lipofuscin-like lipopigments. *,**Ratio is calculated considering AF yield of 3:1 for NAD(P)H in the respective bound and free state (Salmon *et al.*, 1982). **Redox ratio is calculated in terms of (flavins)/(NAD(P)Htotal + flavins), from Kirkpatrick *et al.*, 2005.**

fraction ranging from less than 10% to about 20%. The calculation of the real emission values of each single fluorophore indicates that, independently from the kind of cell considered within each sample, iPS cells in comparison to EBs cells show a greater content of NAD(P)H in parallel with higher NAD(P)$H_{bound/free}$ and lower redox ratio values (Figure 3 A-B). The contribution of lipofuscin-like lipopigments is less than a half in iPS cells with respect to EBs (Figure 3 C), and porphyrins are in general about 1%, except for a contribute for about 4% in the cells localizing at the periphery of EBs (*data not shown*).

Imaging of iPS and EB cells

Images recorded under the near UV excitation from living iPS cells and EBs show fluorescent cytoplasms around dark nuclei. The cytoplasmic AF patterns are characterized by a low and diffuse signal and distinct bluish bright particles, more numerous, evenly distributed and of comparable size in iPS cells than in EBs. Particles with a yellowish and brighter emission signal, a more variable size and uneven distribution can be also observed, more frequently in EBs than in iPS cells (Figure 4).

Discussion

Studies on the role of cell redox balance in the modulation of stemness status and differentiation have recently brought attention to the coenzymes NAD(P)H and flavins, that can act as intrinsic biomarkers because of their participation to energy production, reductive biosynthesis, and antioxidant defense (Uchugonova *et al.*, 2008; Ogasawara and Zhang, 2009; Hamanaka and Chandel, 2010;

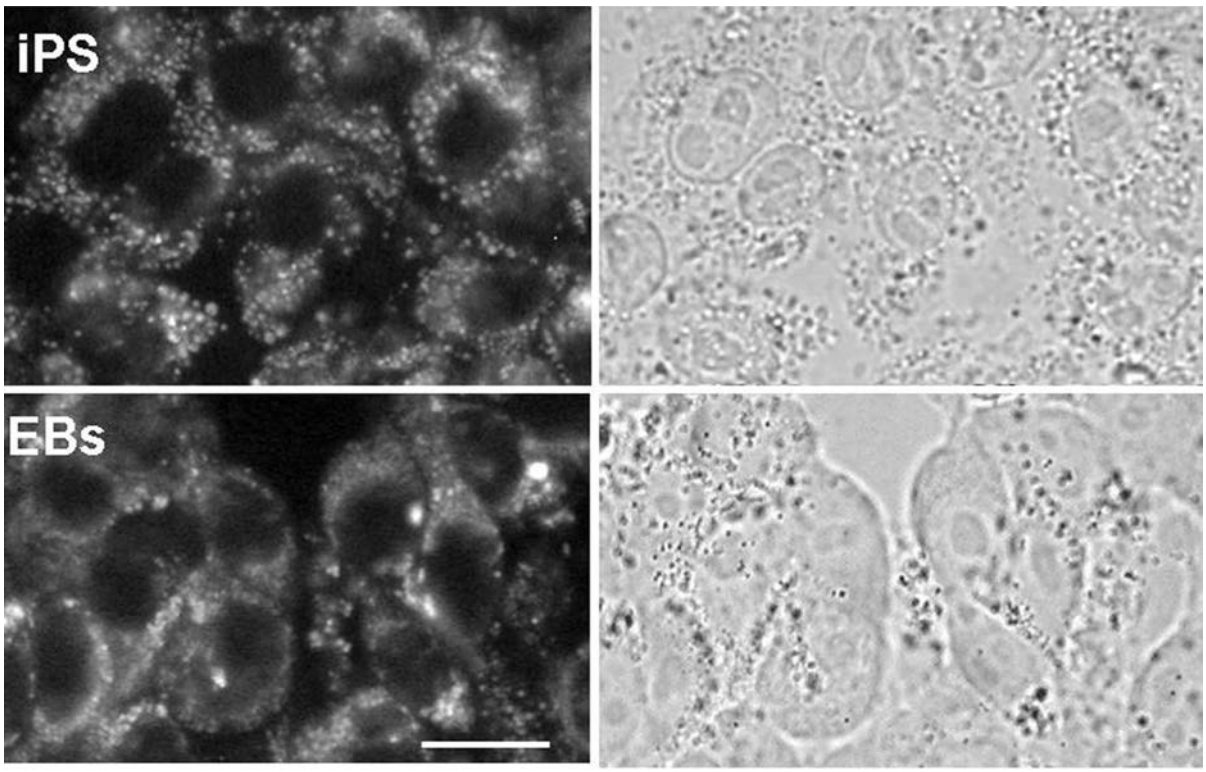

Figure 4. Examples of the AF distribution patterns and corresponding bright field images collected from living iPS cells and EBs. Each pair of images allows to appreciate a cytoplasmic diffuse AF emission signal around the dark nuclei. In comparison with EBs, iPS cells show more numerous bright bluish particles, evenly distributed and of comparable size, ascribable to mitochondria, while more brilliant yellowish granules with variable size and uneven distribution, ascribable to lipofuscin-like lipopigments, are shown by EBs. Bar: 25 µm.

Rice *et al.*, 2010; König *et al.*, 2011; Stringari *et al.*, 2011; Stringari *et al.*, 2012b). Therefore, the AF properties of these coenzymes in terms of signal amplitude, spectral shape and distribution patterns can be expected to reflect possible differences in the engagement of iPS cells and EBs in redox metabolic pathways. Actually, a higher turnover rate between the reduced and oxidized forms of NAD(P)H and flavins in iPS cells with respect to EBs is indicated by their greater content in NAD(P)H, accompanied by a higher NAD(P)H bound/free ratio and a lower redox ratio. These data suggest a still active engagement in aerobic metabolism of iPS cells, consistently with the results previously obtained in normal, young or immortalized fibroblasts (Croce *et al.*, 1999). The direct relationship between the relative increase in NAD(P)H in the bound with respect to the free state following the differentiation from progenitor to adult cell elements is further supported by comparable results on different cellular models undergoing differentiation both in culture and in their native environment (Stringari *et al.*, 2011; Stringari *et al.*, 2012a,b; Santin *et al.*, 2013).

The high redox ratio of EBs, in turn, is likely to be related to a still low turnover rate between reduced and oxidized forms of NAD(P)H and flavins during the switch from anaerobic to aerobic metabolism, with a rising in the engagement of mitochondria in state 3, the high level of oxidative metabolism producing ATP (Li *et al.*, 2009).

The differences in the energetic metabolism engagement suggested by the microspectrofluorometric analysis of our samples are supported by the AF images, able to show more numerous mitochondria in iPS cells than in EBs in the absence of exogenous dyes, because of intrinsic NADH emission. Lipofuscin-like lipopigments contribute to the cell AF emission in the yellow-red region. As a consequence, these fluorophores can be exploited as additional AF biomarkers providing comprehensive information on the presence of waste material accumulated at the intracellular level, as a product of autophagy and oxidative stress damage (Terman *et al.*, 2005; Stolzing *et al.*, 2006; Rice *et al.*, 2010; Rehman, 2010; Terman *et al.*, 2010; Stringari *et al.*, 2012c; Santin *et al.*, 2013). Our results show a much greater amount of lipofuscin-like lipopigments in EBs with respect to iPS cells, in full agreement with the role of autophagic activity providing for the removal of undesired subcellular structures to maintain the cell stemness status (Hernebring *et al.*, 2006; Rehman *et al.*, 2010; Wang *et al.*, 2011; Chen *et al.*, 2012).

Porphyrins, namely Protoporphyrin IX, despite their very small presence can be detected by means of spectral fitting analysis because of their narrow band peaking at 630 nm (Moesta, 2001), distinguishable from the low emission tail of the other fluorophores in the red region. In our samples the highest presence of porphyrins detected in cell clusters of EBs can be explained considering the porphyrin role as intermediates of the synthesis of heme-proteins, such as microsomial or mitochondrial cytochromes. Actually, a direct association between cytochrome *c* synthesis and cardiomyocyte differentiation has been demonstrated (Chen *et al.*, 2012), and an increase in the presence of porphyrins has been found during the transition from anaerobic to aerobic metabolism in mice stem cells (Santin *et al.*, 2013).

Conclusions

The AF results indicate that reprogrammed suine iPS cells do not show a complete recovery of the typical metabolic functions of the undifferentiated status. This finding could be related to the fact that suine iPS cells could not be equivalent to the naive mouse embryoid stem cells (Santin *et al.*, 2013). These results support the ability of AF analysis to assess stem cell differentiation degree and open a new perspective for the application of this technique as a supportive tool to investigate genetic and molecular biomarkers, both in already characterized models or in animal species of interest in veterinary, zootechnology, and more generally in developing research, even when immune-biomarkers are not available (Nowak-Imialek and Niemann, 2012)

Acknowledgments

We thank “Superpig Program” as a project co-financed by Lombardy Region through the “Fund for promoting institutional agreements” for supporting this work. We are also grateful to Prof. Michael Roberts (University of Missouri), for providing the pig iPS cell lines.

References

Aubin JE. Autofluorescence of viable cultured mammalian cells. J Histochem Cytochem 1979;27:36-43.

Balaban RS, Mandel LJ. Optical methods for the study of metabolism in intact cell. In: Forskett JK, Grinstein S, eds. Non-invasive Techniques in Cell Biology. New York USA: Wiley Liss, 1990:213-36.

Bottiroli G, Croce AC. Autofluorescence spectroscopy of cells and tissues as a tool for biomedical diagnosis. Photochem Photobiol Sci 2004;3:189-210.

Chen CT, Hsu SH, Wei YH. Mitochondrial bioenergetic function and metabolic plasticity in stem cell differentiation and cellular reprogramming. Biochim Biophys Acta 2012;1820:571-6.

Cherry AB, Daley GQ. Reprogramming cellular identity for regenerative medicine. Cell 2012;148:1110-22.

Croce AC, Ferrigno A, Vairetti M, Bertone R, Freitas I, Bottiroli G. Autofluorescence properties of isolated rat hepatocytes under different metabolic conditions. Photochem Photobiol Sci 2004;3:920-6.

Croce AC, Spano A, Locatelli D, Barni S, Sciola L, Bottiroli G. Dependence of fibroblast autofluorescence properties on normal and transformed conditions. Role of the metabolic activity. Photochem Photobiol 1999;69:364-74.

Desbaillets I, Ziegler U, Groscurth P, Gassmann M. Embryoid bodies: an in vitro model of mouse embryogenesis. Exp Physiol 2000;85:645-51.

Enver T, Pera M, Peterson C, Andrews PW. Stem cell states, fates, and the rules of attraction. Cell Stem Cell 2009;4:387-97.

Evans MJ, Kaufman MH. Establishment in culture of pluripotential-cells from mouse embryos. Nature 1981;292:154-6.

Ezashi T, Telugu BP, Alexenko AP, Sachdev S, Sinha S, Roberts RM. Derivation of induced pluripotent stem cells from pig somatic cells. Proc Natl Acad Sci U S A 2009;106:10993-8.

Folmes CDL, Dzeja PP, Nelson TJ, Terzic A. Energy metabolism plasticity enables stemness programs. Ann N Y Acad Sci 2012;1254:82-9.

Hamanaka RB, Chandel NS. Mitochondrial reactive oxygen species regulate cellular signaling and dictate biological outcomes. Trends Biochem Sci 2010;35: 505-3.

Hernebring M, Brole´n G, Aguilaniu H, Semb H, Nystro T. Elimination of damaged proteins during differentiation of embryonic stem cells. PNAS 2006;103: 7700-5.

Kahler DJ, Ahmad FS, Ritz A, Hua H, Moroziewicz DN, Sproul AA, et al. Improved methods for reprogramming human dermal fibroblasts using fluorescence activated cell sorting. PLoS One 2013;8:e59867.

Kirkpatrick ND, Zou C, Brewer MA, Brands WR, Drezek RA, Utzinger U. Endogenous fluorescence spectroscopy of cell suspensions for chemopreventive drug monitoring. Photochem Photobiol 2005;81:125-34.

König K, Uchugonova A, Gorjup E. Multiphoton fluorescence lifetime imaging of 3D-stem cell spheroids during differentiation. Microsc Res Tech 2011;74:9-17.

Kunz WS. Spectral properties of fluorescent flavoproteins of isolated rat liver mitochondria. FEBS 1986;195:92-6.

Li LZ, Zhou R, Xu HN, Moon L, Zhong T, Kim EJ, et al. Quantitative magnetic resonance and optical imaging biomarkers of melanoma metastatic potential. Proc Natl Acad Sci USA 2009; 106:6608-13.

Marquardt DW. An algorithm for least-squares estimation of non-linear parameters. J Soc Indust Appl Math 1963;11:431-41.

Moesta KT, Ebert B, Handke T, Nolte D, Nowak C, Haensch WE, et al. Protoporphyrin IX occurs naturally in colorectal cancers and their metastases. Cancer Res 2001;61:991-9.

Nagano K, Yoshida Y, Isobe T. Cell surface biomarkers of embryonic stem cells. Proteomics 2008;8:4025-35.

Nowak-Imialek M, Niemann H. Pluripotent cells in farm animals: state of the art and future perspectives. Reprod Fertil Dev 2012;25:103-28.

Ogasawara MA, Zhang H. Redox regulation and its emerging roles in stem cells and stem-like cancer cells. Antioxid Redox Signal 2009;11:1107-22.

Ramanujam N. Fluorescence spectroscopy in vivo. In: Meyers RA, ed. Encyclopedia of analytical chemistry. Chichester UK: John Wiley and Sons, 2000:20-56.

Rehman J. Empowering self-renewal and differentiation: the role of mitochondria in stem cells. J Mol Med 2010;88:981-6.

Rice WL, Kaplan DL, Georgakoudi I. Two-photon microscopy for non-invasive, quantitative monitoring of stem cell differentiation. PLoS One 2010;5:e10075.

Salmon JM, Kohen E, Viallet P, Hirscheberg JG, Wouters AW, Kohen C, et al. Microspectrofluorometric approach to the study of free/bound NAD(P)H ratio as metabolic indicator in various cell types. Photochem Photobiol 1982;36:585-93.

Santin G, Paulis M, Vezzoni P, Pacchiana G, Bottiroli G, Croce AC. Autofluorescence properties of murine embryonic stem cells during spontaneous differentiation phases. Lasers Surg Med 2013;45:597-607.

Stolzing A, Sethe S, Scutt AM. Stressed stem cells: temperature response in aged mesenchymal stem cells. Stem Cells Dev 2006;15:478-87.

Stringari C, Cinquin A, Cinquin O, Digman MA, Donovan PJ, Gratton E. Phasor approach to fluorescence lifetime microscopy distinguishes different metabolic states of germ cells in a live tissue. Proc Natl Acad

Sci U S A 2011;108:13582-7.
Stringari C, Edwards RA, Pate KT, Waterman ML, Donovan PJ, Gratton E. Metabolic trajectory of cellular differentiation in small intestine by Phasor Fluorescence Lifetime Microscopy of NADH. Sci Rep 2012a;2:568. doi: 10.1038/srep00568.
Stringari C, Nourse JL, Flanagan LA, Gratton E. Phasor fluorescence lifetime microscopy of free and protein-bound NADH reveals neural stem cell differentiation potential. PLoS One 2012b;7:e48014.
Stringari C, Sierra R, Donovan PJ, Gratton E. Label-free separation of human embryonic stem cells and their differentiating progenies by phasor fluorescence lifetime microscopy. J Biomed Opt. 2012c;17:046012-1-11, doi: 10.1117/1.JBO.17.4.046012.
Terman A, Brunk UT. Autophagy in cardiac myocyte homeostasis, aging, and pathology. Cardiovasc Res. 2005;68:355-65.
Terman A, Gustafsson B, Brunk UT. Mitochondrial damage and intralysosomal degradation in cellular aging. Mol Aspects Med 2006;27:471-82.
Terman A, Kurz T, Navratil M, Arriaga EA, Brunk UT. Mitochondrial turnover and aging of long-lived postmitotic cells: the mitochondrial–lysosomal axis theory of aging. Antioxid Redox Signal 2010;12:503-35.
Uchugonova A, König K. Two-photon autofluorescence and second-harmonic imaging of adult stem cells J Biomed Opt 2008;13:054068. doi:10.1117/1.3002370.
Wang J, Alexander P, McKnight SL. Metabolic specialization of mouse embryonic stem cells. Cold Spring Harb Symp Quant Biol 2011;76:183-93.
Welling M, Geijsen N. Uncovering the true identity of naïve pluripotent stem cells. Trends Cell Biol 2013;23:442-8.
Williams RL, Hilton DJ, Pease S, Willson TA, Stewart CL, Gearing DP, Wagner EF, Metcalf D, Nicola NA, Gough NM. Myeloid leukaemia inhibitory factor maintains the developmental potential of embryonic stem cells. Nature 1988;336:684-7.
Wolman M. Lipid pigments (chromolipids): their origin, nature and significance. Pathobiol Ann 1980;10:253-67.
Yamanaka S. A fresh look at iPS cells. Cell 2009;137:13-7.

I VANTAGGI DEI SOCI SISM

Essere Soci SISM (Società Italiana Scienze Microscopiche) vuol dire far parte di una Società Scientifica che, nata dalla consolidata tradizione scientifica della SIME (Società Italiana di Microscopia Elettronica), opera con uno spirito di forte dinamicità nei diversi settori della Microscopia, è sempre attenta alle continue evoluzioni tecniche e scientifiche in ambito Biologico, Biomedico e in Scienza dei Materiali e ha voluto fare della integrazione tra Ricercatori, Tecnici e quanti sono interessati alle applicazioni ed al progresso delle Scienze Microscopiche il suo obiettivo costante. La Società promuove Congressi Scientifici a livello nazionale ed internazionale, organizza e sponsorizza Scuole, Corsi teorico-pratici, Workshops, Seminari su specifici temi di particolare interesse e/o attualità per favorire l'aggiornamento teorico-applicativo di ricercatori, operatori professionali e personale specializzato delle aziende del settore.
Essere Soci SISM vuol dire:

- far parte dell'EMS (European Microscopy Society, www.eurmicsoc.org) e usufruire delle opportunità offerte dalla Società Europea in termini di informazioni, aggiornamenti, Corsi e Congressi a cui si può partecipare con quote ridotte;
- avere la possibilità di ricevere la rivista semestrale Microscopie che contiene informazioni riguardanti non solo le attività della Società, ma anche le novità che possono offrire le Ditte legate al settore, recensioni su pubblicazioni di interesse per i microscopisti, articoli scientifici e contributi dai diversi Centri di Microscopia che, diffusi su territorio nazionale, offrono grandi potenzialità in termini di strumentazioni e di competenze scientifiche facilmente condivisibili tra i Soci SISM;
- essere informati delle attività, Congressuali e non, che coinvolgono il mondo della microscopia in tutti i suoi aspetti;
- partecipare con quote vantaggiose a tutte le attività della Società;
- partecipare con quote vantaggiose alle iniziative accreditate secondo il progetto ECM (Educazione Continua in Medicina);
- avere la possibilità, per i giovani non strutturati, di usufruire di premi e borse di studio intese a favorire la partecipazione a Congressi di Microscopia nazionali ed internazionali e a premiare la ricerca svolta;
- avere libero accesso, a richiesta, a materiale didattico e scientifico prodotto dalla Società su argomenti di particolare attualità e interesse;
- avere la possibilità, per i Soci che siano promotori di attività di spin-off, di partecipare, con quote vantaggiose, alle iniziative della Società.

In conclusione, essere Soci della SISM vuol dire far parte di una Comunità di Microscopisti attiva, dinamica e in continua evoluzione non solo su scala nazionale, ma anche in un contesto europeo.
Per maggiori informazioni si prega di consultare il sito all'indirizzo **www.sism.it.**

ISTRUZIONI AGLI AUTORI

I manoscritti devono rispecchiare, nel loro contenuto, le principali aree di interesse scientifico della Società (biologia, medicina, ambiente e scienza dei materiali). Saranno considerati per la pubblicazione lavori di carattere sia metodologico che applicativo.
Gli Autori devono inviare, per e-mail al Direttore Responsabile, il manoscritto, in lingua inglese, almeno 40 giorni prima della pubblicazione della rivista stessa. Gli Autori saranno avvisati dell'accettazione del lavoro, sempre via e-mail, dopo che i componenti del Consiglio Direttivo avranno revisionato il manoscritto e suggerito eventuali modifiche.
Il manoscritto, completo di tabelle e didascalie, dovrà essere fornito in un unico file in formato .DOC, mentre le figure dovranno essere in formato .TIF o .JPG ed avere una risoluzione pari o superiore a 300 dpi alle dimensioni finali di stampa.
La prima pagina deve riportare il titolo del lavoro, il nome ed il cognome degli Autori, con relative affiliazioni, e l'indirizzo completo dell'Autore di riferimento. La seconda pagina deve contenere il riassunto e cinque parole chiave. Il lavoro deve essere diviso in paragrafi secondo il seguente ordine: Introduzione, Materiali e Metodi, Risultati, Discussione e Bibliografia. Quest'ultima deve essere redatta in ordine alfabetico e secondo lo schema sotto riportato:

- Montone A, Grbovic Novakovic J, Vittori Antisari M, Bassetti A, Bonetti E, Fiorini AL, *et al.* Nano-micro MgH2-Mg2NiH4 composites: Tayloring a multichannel system with selected hydrogen sorption properties. Int J Hydrogen Energy 2007;32:2926-34.
- Beridze T. Satellite DNA. Springer-Verlag, Berlin, 1982.
- Mc Conkey DJ, Orrenius S. Cellular signaling in thymocyte apoptosis. In: Tomei LD, Cope FO, eds. Apoptosis: The Molecular Basis of Cell Death. Curr Comm Cell and Mol Biol, vol. 3. Cold Spring Harbor Laboratory Press, New York, 1991, pp. 227-46.

Ai lavori di uno stesso autore pubblicati nello stesso anno deve essere aggiunto un suffisso dopo la data (a, b, etc).
Nel testo, i riferimenti bibliografici vanno riportati tra parentesi e devono contenere il cognome dell'autore, l'anno di pubblicazione e l'eventuale suffisso. Nel caso di due autori, vengono riportati entrambi i cognomi; nel caso di tre o più autori, va riportato il cognome del primo autore seguito da "*et al.*".
Le didascalie delle figure e le tabelle devono essere allegate alla fine del testo, su pagine separate. Le figure devono essere numerate progressivamente nello stesso ordine in cui compaiono nel manoscritto. Le fotografie saranno stampate a colori solo se necessario e il costo sarà addebitato agli Autori.
In base a criteri di rilevanza scientifica e qualità artistica, potrà essere scelta per la copertina una figura dai lavori accettati per la pubblicazione.

TARIFFE INSERZIONI PUBBLICITARIE

La rivista Microscopie è una pubblicazione a carattere tecnico-scientifico edita dalla Società Italiana Scienze Microscopiche (SISM) che viene distribuita a tutti i soci. La rivista ha periodicità semestrale ed è stampata in b/n in formato A4 con copertina a colori. A pagamento possono essere inserite pagine interne a colori.
Le tariffe per le inserzioni pubblicitarie sono le seguenti:

Pagina interna b/n	€ 400,00
Pagina interna colore	€ 600,00
Seconda o terza di copertina (colore)	€ 800,00
Quarta di copertina (colore)	€ 1000,00

I prezzi si intendono per singola pagina, IVA esclusa.

Il materiale pubblicitario, di elevata qualità, deve essere fornito su supporto digitale e deve essere inviato almeno 15 giorni prima della pubblicazione della rivista al seguente indirizzo:

Manuela Malatesta
Dipartimento di Scienze Neurologiche e del Movimento, Sezione di Anatomia e Istologia
Università degli Studi di Verona strada Le Grazie, 8 37134 Verona
Tel. +39.045.8027157/8425115
E-mail: manuela.malatesta@univr.it

Date di pubblicazione della rivista: 15 Marzo e 15 Settembre.

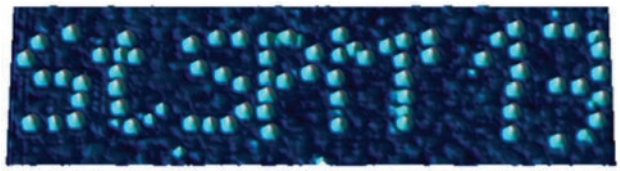

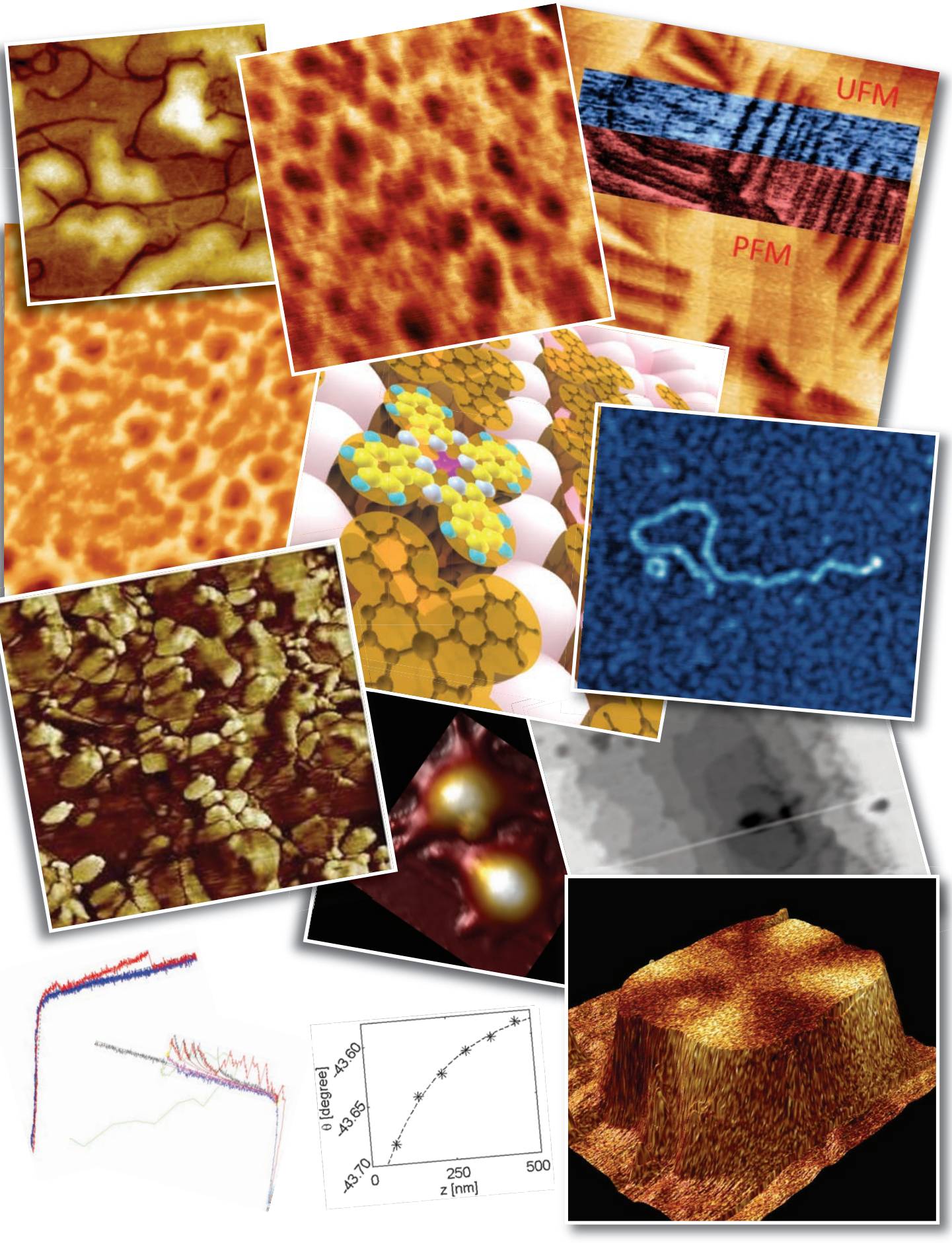
UFM
PFM
θ [degree]
-43.60
-43.65
-43.70
0
250
500
z [nm]